

## REVIEW

[View Article Online](#)  
[View Journal](#) | [View Issue](#)



Cite this: *Nanoscale Adv.*, 2019, **1**, 4560

## Advances in nanomaterial application in enzyme-based electrochemical biosensors: a review

I. S. Kucherenko,  <sup>ab</sup> O. O. Soldatkin, <sup>ac</sup> D. Yu. Kucherenko, <sup>a</sup> O. V. Soldatkina<sup>cd</sup> and S. V. Dzyadevych<sup>ac</sup>

Electrochemical enzyme-based biosensors are one of the largest and commercially successful groups of biosensors. Integration of nanomaterials in the biosensors results in significant improvement of biosensor sensitivity, limit of detection, stability, response rate and other analytical characteristics. Thus, new functional nanomaterials are key components of numerous biosensors. However, due to the great variety of available nanomaterials, they should be carefully selected according to the desired effects. The present review covers the recent applications of various types of nanomaterials in electrochemical enzyme-based biosensors for the detection of small biomolecules, environmental pollutants, food contaminants, and clinical biomarkers. Benefits and limitations of using nanomaterials for analytical purposes are discussed. Furthermore, we highlight specific properties of different nanomaterials, which are relevant to electrochemical biosensors. The review is structured according to the types of nanomaterials. We describe the application of inorganic nanomaterials, such as gold nanoparticles (AuNPs), platinum nanoparticles (PtNPs), silver nanoparticles (AgNPs), and palladium nanoparticles (PdNPs), zeolites, inorganic quantum dots, and organic nanomaterials, such as single-walled carbon nanotubes (SWCNTs), multi-walled carbon nanotubes (MWCNTs), carbon and graphene quantum dots, graphene, fullerenes, and calixarenes. Usage of composite nanomaterials is also presented.

Received 8th August 2019  
Accepted 28th October 2019

DOI: 10.1039/c9na00491b  
[rsc.li/nanoscale-advances](http://rsc.li/nanoscale-advances)

<sup>a</sup>Department of Biomolecular Electronics, Institute of Molecular Biology and Genetics of the National Academy of Sciences of Ukraine, Zabolotnogo Street 150, Kyiv, 03143, Ukraine. E-mail: kucherenko.i.s@gmail.com

<sup>b</sup>Department of Mechanical Engineering, Iowa State University, Ames, Iowa 50011, USA

<sup>c</sup>Institute of High Technologies, Taras Shevchenko National University of Kyiv, Volodymyrska Street 64, Kyiv, 01003, Ukraine

<sup>d</sup>F. D. Ovcharenko Institute of Biocolloidal Chemistry, Acad. Vernadskoho Blvd. 42, Kyiv, 03142, Ukraine



From left to right : O. O.  
Soldatkin, S.V. Dzyadevych, D. Yu  
Kucherenko, I. S. Kucherenko, and O.V. Soldatkina

### 1. Introduction

Biosensors are a group of state-of-the-art analytical devices involving a biorecognition material in close contact with a transducer.<sup>1</sup> An important benefit of biosensors is their significantly lower cost compared to alternative and commonly used methods. Additionally, biosensors are usually portable and easy-to-use, therefore their development is an urgent task of biotechnology and analytical chemistry.

Oleksandr Soldatkin, Sergei Dzyadevych, Daria Kucherenko, Ivan Kucherenko, and Olga Soldatkina are researchers at the Department of Biomolecular Electronics of the Institute of Molecular Biology and Genetics of the National Academy of Sciences of Ukraine (Kyiv, Ukraine). S. Dzyadevych is also working as a deputy director of the same institute since 2019. They received PhD degrees in biotechnology. They are developing electrochemical enzyme-based biosensors for medical, research, and industrial applications. The biosensors are based on amperometric, ISFET, and conductometric transducers and immobilized enzymes. Target molecules include carbohydrates (sucrose, maltose), biomarkers (creatinine kinase, urea, creatinine, lactate), toxins (mycotoxins, heavy metals, pesticides), and various small molecules (ATP, glutamate, dopamine).

Table 1 Comparison of NMs according to the properties important for enzyme-based biosensors<sup>a</sup>

Nanomaterial	High conductance	High adsorption capability	Catalysis of reactions	Other features
AuNPs	Yes	No	No	Possibility of thiol bonds formation
PtNPs	Yes	No	$H_2O_2$ decomposition	No
AgNPs	Yes	No	No	No
PdNPs	Yes	No	$H_2O_2$ decomposition	Relatively cheap
Zeolites	No	Yes	No	No
Inorganic QDs	No	No	No	Semiconductor and optical properties
CNTs	Yes	No	No	No
Organic QDs	No	No	NADH oxidation	Optical properties
Graphene and derivatives	Yes	No	No	No
Fullerenes	Yes	No	No	No
Calixarenes	No	No	No	Specific binding of small molecules

<sup>a</sup> AgNPs – silver nanoparticles; AuNPs – gold nanoparticles; CNTs – carbon nanotubes; NADH – reduced nicotinamide adenine dinucleotide; PdNPs – palladium nanoparticles; PtNPs – platinum nanoparticles; QDs – quantum dots.

The spectrum of biosensors applications is quite wide. Supposedly, in future biosensors will be widely used in medicine, agriculture, control of various biotechnological processes, environmental monitoring of toxic compounds and other areas. Electrochemical enzyme-based biosensors are one of the most advanced and commercially successful bioanalytical devices because of a high catalytic activity and selectivity of enzymes, as well as commercial availability of purified enzymes. However, traditional enzyme-based biosensors have limited sensitivity, selectivity, and stability, thus different approaches to improvement of the biosensors are considered.

A new promising trend in biosensorics is the use of nano-scale materials of various types, which have unique physical and chemical properties. Nanomaterials (NMs), the substances with the size of structural elements of 1–100 nm, significantly differ from similar macro-scale materials. In biosensors, NMs are used to improve the basic analytical characteristics of biosensors, such as sensitivity, limit of detection (LOD), linear detection range, selectivity, reproducibility, stability, response time, *etc.*<sup>2</sup> Unique properties of NMs, in particular, a high surface-to-volume ratio, ensure significant increase in the sensitive surface of the transducer and more effective enzyme immobilization. Additionally, NMs are characterized by high electrical conductivity, magnetic properties, catalytic activity, *etc.*, which are important for biosensors.<sup>3</sup> Moreover, surface of NMs can be easily modified with different chemical groups,<sup>4,5</sup> which is essential for the interaction with biomaterial in biosensors and other biotechnological assays.<sup>6</sup> Doped NMs also provide a flexible way to obtain highly effective sensors.<sup>7</sup> A perspective approach is the synthesis of NMs that form colored complexes with their targets – such complexes can be observed with the naked eye.<sup>8</sup> Separation of molecules in complex matrixes can be also achieved using NMs.<sup>9–12</sup>

By the chemical structure, NMs can be divided into organic and inorganic. Inorganic NMs include metals and their oxides, quantum dots, zeolites, *etc.*; fullerenes, carbon nanotubes (CNTs), graphene and graphene oxide, calixarenes, *etc.* are

organic NMs.<sup>13</sup> Inorganic NMs are characterized by relatively simple synthesis; they catalyze some electrochemical reactions,<sup>14,15</sup> and participate in acceleration of electron transfer. Organic NMs are characterized by the properties, which contribute to the amplification of the electrochemical signal and ensure a high degree of biocompatibility.<sup>6,16</sup> Both types of NMs are useful in the development of electrochemical sensors.<sup>17</sup> More exotic NMs such as semiconductor or composite NMs are also studied.<sup>18</sup> General comparison of NMs is presented in Table 1.

An alternative classification of NMs is based on their dimensions.<sup>19</sup> NMs are divided into 0D clusters and particles, 1D nanowires and nanotubes, 2D films, and 3D structures. However, in the present review we use the chemical classification of NMs.

To improve sensors' analytical characteristics, nanoparticles can be used in different ways. They can be either co-immobilized with the enzymes or integrated into the transducer surface; some nanoparticles can be used as a selective element of chemosensors.<sup>20–24</sup> Thus, depending on the objective it is possible to obtain required parameters of the sensors by appropriate choice of NMs and procedure of their application.

The utilization of nano- and micro-materials to improve the analytical characteristics of biosensors is one of the major trends of analytical biotechnology.

Here, we reviewed the recent applications of various types of NMs in electrochemical enzyme-based biosensors for the detection of environmental pollutants, food contaminants, and clinical biomarkers. Additionally, we discussed the benefits and limitations of using NMs for analytical purposes.

## 2. Methods of embedding nanomaterials in the enzyme-based biosensors

An electrochemical transducer can be modified with NMs before the biomaterial immobilization, or NMs can be



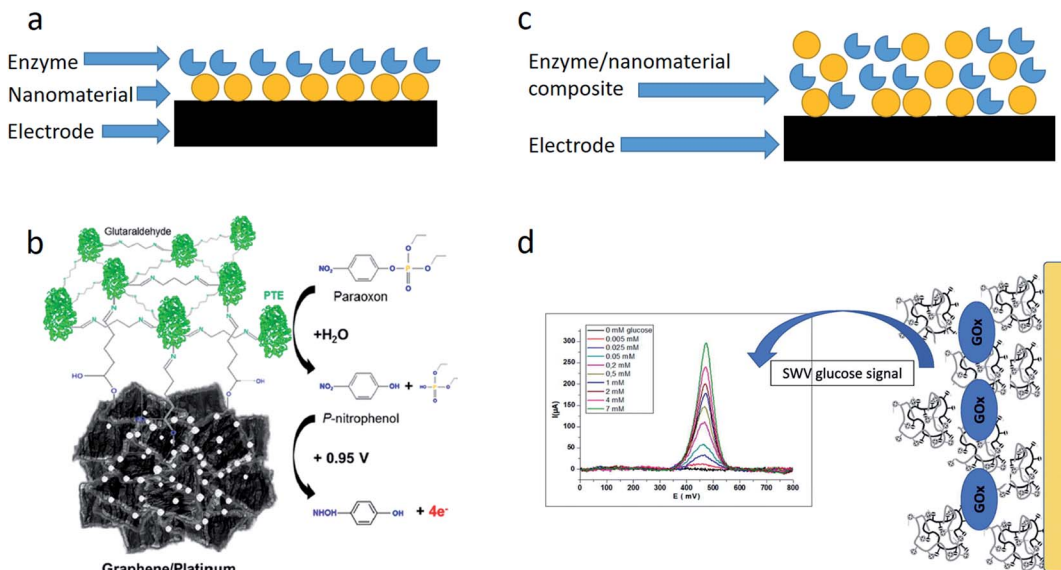


**Fig. 1** Ways of embedding NMs in the enzyme-based biosensors. (a) Enzyme immobilization on the NM-modified electrode. (b) Schematic of the biosensor based on phosphotriesterase (PTE) immobilized via glutaraldehyde on the graphene surface with platinum nanoparticles. Reprinted with permission from J. A. Hondred, J. C. Breger, N. J. Alves, S. A. Trammell, S. A. Walper, I. L. Medintz and J. C. Claussen, Printed Graphene Electrochemical Biosensors Fabricated by Inkjet Maskless Lithography for Rapid and Sensitive Detection of Organophosphates, *ACS Applied Materials & Interfaces*, 2018, **10**, 11125–11134. Copyright 2018 American Chemical Society.<sup>25</sup> (c) Enzyme/NM co-immobilization on the electrode. Reprinted from *Material Science and Engineering: C*, 95, I. Rassas, M. Braiek, A. Bonhomme, F. Bessueille, G. Rafin, H. Majdoub, and N. Jaffrezic-Renault, Voltammetric glucose biosensor based on glucose oxidase encapsulation in a chitosan-kappa-carrageenan polyelectrolyte complex, 152–159, Copyright (2018), with permission from Elsevier.<sup>26</sup>

immobilized together with the bioreceptor component (Fig. 1). In the first case, NMs are synthesized directly on the transducer surface by applying constant or variable voltage, and then the enzymes are adsorbed on NMs or immobilized in any other way.

Enzymes can be easily immobilized directly onto the nanoparticles, since enzymes have many functional groups such as carboxylic ( $-\text{COOH}$ ), amino ( $-\text{NH}_2$ ), thiol ( $-\text{SH}$ ), etc. NMs with hydrophobic or charged sites on their surface, which can interact with enzymes, or NMs with chemical groups, which are able to bind to the corresponding enzyme groups, can be the enzymes adsorbents. In the first place, inorganic mesoporous materials are attractive adsorbents since they have a large surface area of the crystal and can carry various chemical groups, such as zeolites and mesoporous silicon spheres.<sup>27</sup>

Alternatively, NMs are synthesized separately and mixed with the enzyme solution prior to immobilization. This approach can be used for incorporation of NMs, which do not adsorb the enzymes. However, many NMs (especially organic ones) do not dissolve in aqueous solutions at all or easily aggregate in them, thus an addition of surfactants or other stabilizers to the resulting NM/enzyme mixture is often required. The auxiliary compounds should be carefully selected, since they can worsen the enzyme activity.

It is possible to combine both options of NMs incorporation, first immobilizing the enzyme on NM and then attaching the enzyme/NM composite to the electrode.

The application of NMs in biosensors results in:

- Enhancement of the transfer of electrons, which are formed or used in the enzymatic reaction, between the transducer surface and the enzyme;
- An increase of the sensor sensitive surface and thus enables immobilization of a larger amount of enzyme molecules;
- Improvement of enzyme stability;
- Catalysis of additional chemical reactions.<sup>28</sup>

### 3. Inorganic nanomaterials in enzyme-based biosensors

The most widespread inorganic NMs are nanosized particles of metals and metal oxides ( $\text{TiO}_2$ ,  $\text{Al}_2\text{O}_3$ ,  $\text{Fe}_2\text{O}_3$ ,  $\text{ZrO}_2$ ,  $\text{MoO}_3$ , and  $\text{CeO}_2$ ), quantum dots and zeolites. In biosensors, metal nanoparticles are commonly used due to their unique physical and chemical properties.<sup>29–31</sup>

There are two groups of methods of simple production of inorganic NMs – physical (fragmentation of the initial material to nanoscaled particles) and chemical (synthesis from precursors). The synthesized nanoparticles usually are more uniform compared to fragmented ones.

The advantages of inorganic NMs are simple production, the possibility of various surface modifications, catalysis of chemical reactions, acceleration of the electron transfer, biocompatibility, and improvement of conditions of enzyme

immobilization. It makes NMs promising in the development of electrochemical enzyme-based biosensors.<sup>17</sup> Some examples of the application of inorganic NMs are given in Table 2.

### 3.1. Gold nanoparticles

Gold nanoparticles (AuNPs) are widely utilized in enzyme-based biosensors. AuNPs are highly conductive and biocompatible, and their distinctive feature is the formation of strong thiol bonds between organic substances (*i.e.*, cysteine residues of enzymes) and nanoparticles.<sup>28</sup> Thus, the nanoparticles form a suitable microenvironment for the enzyme immobilization. The Enzyme activity can be significantly enhanced by immobilization onto AuNPs.<sup>44</sup>

The researchers proposed a biosensor for the determination of organophosphorus pesticide formetanate, using laccase immobilized onto a gold electrode, modified with electrochemically deposited AuNPs.<sup>40</sup> Detection was based on inhibition of the laccase activity by the pesticide. The biosensor appeared to be highly sensitive to the pesticide (LOD – 95 nM), and was successfully used to identify this pesticide in fruits.

A conductometric biosensor was developed for the hydrogen peroxide determination based on horseradish peroxidase immobilized in a chitosan film with and without 11 nm AuNPs.<sup>45</sup> Interestingly, the addition of nanoparticles resulted in a decrease of the biosensor response, which, due to the authors, occurred because of the difference in the oxidative states of AuNPs and the active center of horseradish peroxidase.

A potentiometric biosensor for the determination of pesticide glyphosate was proposed; it was based on urease immobilized with AuNPs 2.54 nm in diameter.<sup>46</sup> Glyphosate inhibited urease, which led to a decrease in the response of ammonium-sensitive ion-selective electrode. The linear range of the glyphosate detection was 0.5–50 ppm (3–300  $\mu$ M), LOD – 0.5 ppm (3  $\mu$ M).

The biosensor, recently proposed for determination of the protein kinase A activity, was based on horseradish peroxidase, antibodies (IgG) and AuNPs.<sup>47</sup> The use of nanoparticles reduced the working potential to 0.08 V.

The change in the diameter of AuNPs due to their aggregation or growth during synthesis causes the variation in optical properties of their suspension (an adsorption of light with a wavelength from 400 to 700 nm increases accompanied by a change in color). This phenomenon can be used to visualize a certain reaction. In particular, a biosensor for the colorimetric determination of acetylcholinesterase inhibitors was proposed.<sup>48</sup> In the absence of inhibitors, the enzyme catalyzed the cleavage of acetylthiocholine to acetic acid and thiocholine. The latter reduced  $\text{AuCl}^{4-}$ , which led to an increase in the AuNPs diameter and the change in the suspension color from a weakly pink to purple. In the presence of acetylcholinesterase inhibitors in the sample, neither the growth of 2–3 nm AuNPs nor the corresponding change of solution color was observed.

Other platinum nanostructures can be also used in enzyme-based biosensors for effective  $\text{H}_2\text{O}_2$  detection. For example, fractal nanoplatinum structures were synthesized by four different methods and used for the glucose oxidase (GOx) immobilization.<sup>49</sup> The developed amperometric biosensor demonstrated very high sensitivity to hydrogen peroxide ( $3335 \pm 305 \mu\text{A cm}^2 \text{ mM}^{-1}$ ), but sensitivity to glucose was notably lower ( $155 \pm 25 \mu\text{A cm}^2 \text{ mM}^{-1}$ ). The biosensor response to glucose was rapid ( $2.0 \pm 0.6$  s). According to the authors, in general the analytical characteristics were not worse or even exceeded those of other glucose biosensors based on GOx and NMs.

### 3.2. Platinum nanoparticles

Platinum nanoparticles (PtNPs) differ from nanoparticles of other metals by the ability to catalyze decomposition of

Table 2 Examples of electrochemical biosensors based on enzymes and inorganic NMs<sup>a</sup>

Sensitive element	Analyte	Method of detection	LOD	Real sample	Ref.
Acetylcholine esterase/ZnO/SPE	Paraoxon	CA	0.035 ppm	N/D	32
Acetylcholine esterase/ $\text{Fe}_3\text{O}_4\text{NP/CNT/ITO}$	Malathion, chlorpyrifos, monocrotophos, endosulfan	CV	0.1 nM	Cabbage, onions, spinach, soil	33
Cholesterol esterase/ cholesterol oxidase/ quantum dots CdS/chitosan	Cholesterol and cholesterol esters	CV	0.47 mM	N/D	34
Glucose oxidase/CNT/PtNP/GCE	Glucose	CA	6 $\mu\text{M}$	N/D	35
Glucose oxidase/PdNP/CNT	Glucose	CV	150 $\mu\text{M}$	N/D	36
Glutamate oxidase/CNT/AuNP/AuE	Glutamate	CA	1.6 $\mu\text{M}$	Human blood serum	37
Horseradish peroxidase/TiO <sub>2</sub> NT	Hydrogen peroxide	CA	0.1 $\mu\text{M}$	N/D	38
Horseradish peroxidase/TiO <sub>2</sub> NT	Hydrogen peroxide	Detection of photocurrent	0.7 nM	N/D	39
Laccase/AuNP/AuE	Formetanate	SWV	0.095 $\mu\text{M}$	Mango, grapes	40
Lactate oxidase/AgNP	Lactate	CA	1 mM	N/D	41
Tyrosinase/graphene/PtNP/GCE	Chlorpyrifos, profenofos, malathion	CA	0.2 ppb, 0.8 ppb, 3 ppb	N/D	42
Tyrosinase/quantum dots CdS/chitosan	Phenol compounds	CA	0.3 nM	Water	43

<sup>a</sup> AuE – gold electrode; CA – chronoamperometry; CNT – carbon nanotubes; CV – cyclic voltammetry; GCE – glassy carbon electrode; ITO – indium tin oxide; N/D – no data; NP – nanoparticle; NT – nanotube; SPE – screen-printed electrode; SWV – square wave voltammetry.



hydrogen peroxide ( $\text{H}_2\text{O}_2$ ), a common product of oxidative reactions. An oxidation or reduction of hydrogen peroxide results in the formation or adsorption of electrons, which can be registered by amperometric methods. Basically, hydrogen peroxide decomposes spontaneously, but the catalyst significantly accelerates this reaction and increases the biosensor response. Though conventional platinum electrodes have the same catalytic activity, usage of platinum nanoparticles considerably increases the surface area and number of catalytic sites. The electrode modification with platinum nanoparticles can be carried out by chemical reduction, electrochemical and photochemical deposition of platinum compounds (usually  $\text{PtCl}^{6-}$ ). The choice of method for the nanoparticles synthesis defines their chemical inertness, electrical resistance, background current, and catalytic properties.<sup>50-52</sup>

Numerous amperometric biosensors contain oxidases and platinum NMs. For example, the biosensors for the determination of glucose based on GOx and diamond microfibers were compared with the analogues which differed in the addition of PtNPs; the latter demonstrated a significantly higher sensitivity.<sup>53</sup>

An amperometric biosensor based on GOx, co-immobilized with PtNP/SnS<sub>2</sub> composite is described in.<sup>54</sup> Due to the authors, the nanocomposite improved the direct electron transfer between the enzyme and the surface of the glassy carbon electrode, and allowed the potential  $-0.4$  V *vs.* saturated calomel electrode to be used. The biosensor had two linear ranges of glucose determination ( $0.1$ – $1.0$  mM and  $1.0$ – $12$  mM), LOD was  $2.5$   $\mu\text{M}$ .

Although PtNPs are useful in the first place for amperometry, PtNPs were integrated in the potentiometric biosensor for the sulfites determination based on sulfite oxidase, immobilized in the polypyrrole film with PtNPs (Fig. 2).<sup>55</sup> The biosensor was very sensitive to the substrate; the LOD was  $12.4$  nM, the linear range  $0.75$ – $65$   $\mu\text{M}$ , the response time  $3$ – $5$  s.

### 3.3. Silver nanoparticles

The benefits of using silver nanoparticles (AgNPs) in biosensors are similar to those of other metal nanoparticles – enhancement of the matrix conductivity and amplification of the electrochemical signal.

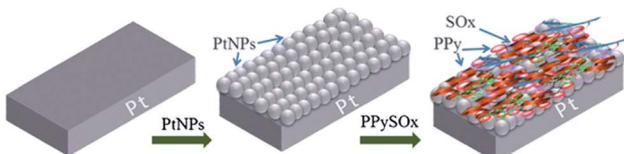


Fig. 2 Preparation of the potentiometric sulfite biosensor: modification of the working electrode surface with PtNPs followed by the immobilization of sulfite oxidase (SOx) in the polypyrrole film. Reprinted by permission from: Springer-Verlag Wien, *Microchimica Acta*, (Potentiometric sulfite biosensor based on entrapment of sulfite oxidase in a polypyrrole film on a platinum electrode modified with platinum nanoparticles, S. B. Adelaju and S. Hussain), © (2016).<sup>55</sup>

An amperometric biosensor developed for the urea determination was based on urease immobilized in a composite matrix containing polyaniline, polyvinyl acetate and AgNPs stabilized in polyvinyl alcohol.<sup>56</sup> For comparison, the characteristics of the biosensor signal were studied without AgNPs. It was found that addition of AgNPs changed the shape of cyclic voltammograms – the cathodic peak (caused by urea addition) became more pronounced, which resulted in more accurate determination of urea concentration.

An amperometric biosensor with a flexible electrode was developed using lactate oxidase and AgNPs.<sup>41</sup> The biosensor was intended for lactate determination in sweat. Linear range of detection was  $1$ – $25$  mM, which coincided with the normal concentrations of lactate in human sweat. Noteworthy, the biosensor operated at a sufficiently high working potential ( $0.65$  V *vs.* Ag/AgCl reference electrode), and the effect of anionic interfering substances was eliminated by the deposition of an additional negatively charged Nafion® membrane.

On the other hand, when developing the amperometric laccase-based biosensor, it was shown that an addition of AgNPs in high concentrations resulted in a 2390-fold decrease of the sensitivity.<sup>57</sup> Such negative experience, though rarely reported, indicates that the amount of nanoparticles should be optimized.

### 3.4. Palladium nanoparticles

Palladium nanoparticles (PdNPs) have attracted more and more attention not only due to their conductive properties and catalytic activity, but also because of lower cost compared to AgNPs or PtNPs.<sup>13</sup> Additionally, PdNPs can catalyze the reactions involving hydrogen peroxide (but probably at a slower rate than PtNPs).

It has been recently shown that a glassy carbon electrode, modified with  $9$  nm PdNPs, effectively reduces hydrogen peroxide at a potential of  $-0.12$  V, which may be useful in the development of amperometric biosensors based on oxidases.<sup>58</sup> The limit of hydrogen peroxide detection was  $0.34$   $\mu\text{M}$ .

The effects of nanoparticles of various metals (gold, platinum, rhodium and palladium) on the performance of superoxide dismutase-based biosensor for determination of aluminum ions were compared.<sup>59</sup> The highest sensitivity was observed with PdNPs, LOD was  $2$   $\mu\text{M}$ .

PdNPs are often used in combination with other NMs. For example, the glucose biosensor in ref. 60 was based on GOx, PdNPs, and multi-walled carbon nanotubes (MWCNTs). The biosensor could operate in the working potential range from  $-0.2$  to  $-0.5$  V. Furthermore, PdNPs improved the biosensor stability. The biosensor was used for glucose determination in honey and blood serum. In a similar biosensor PdNPs were used along with graphene and chitosan.<sup>61</sup> Additionally, the sensor based on a reduced graphene oxide (rGO), *tert*-nonyl mercaptan (TNM), and PdNPs was proposed for hydrogen peroxide determination at the potential from  $-0.6$  to  $+0.8$  V (Fig. 3).<sup>62</sup> Linear range of  $\text{H}_2\text{O}_2$  detection was up to  $12$  mM and LOD was  $2.5$   $\mu\text{M}$ .



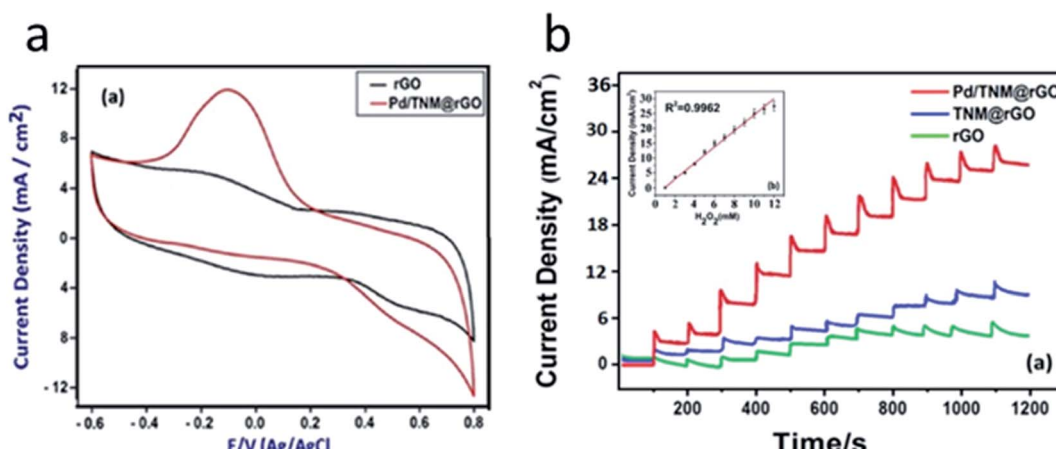


**Fig. 3** Operation of the amperometric sensor for hydrogen peroxide detection. (a) Cyclic voltammograms obtained with rGO electrode and PdNP/TNM/rGO in 0.1 M PBS, with 5 mM  $\text{H}_2\text{O}_2$ . (b) Amperometric responses of rGO, TNM@rGO, and Pd/TNM@rGO sensor to 1–12 mM  $\text{H}_2\text{O}_2$  in 0.1 M PBS at pH 7.4 at applied potential of  $-0.1\text{ V}$ . Inset: corresponding calibration plot of Pd/TNM@rGO sensor. Reprinted from *Analytica Chimica Acta*, **989**, S. Bozkurt, B. Tosun, B. Sen, S. Akocak, A. Savk, M. F. Ebeoğlu and F. Sen, A hydrogen peroxide sensor based on TNM functionalized reduced graphene oxide grafted with highly monodisperse Pd nanoparticles, 88–94, Copyright (2017), with permission from Elsevier.<sup>62</sup>

### 3.5. Iron oxide nanoparticles

The iron oxide ( $\text{Fe}_3\text{O}_4$ ) NPs catalyze the oxidation of hydrogen peroxide and thus can improve the response of oxidase-based biosensors.<sup>63</sup> Although the catalytic activity of the iron oxide nanoparticles is lower than that of PtNPs and PdNPs, reagents for the  $\text{Fe}_3\text{O}_4$  NPs synthesis are much cheaper. Furthermore, these NPs have magnetic properties and can be attached to the surface of the electrode using external magnetic field. Recently  $\text{Fe}_3\text{O}_4$  NPs were used for creation of biosensors based on GOx<sup>64–66</sup> and acetylcholine esterase/choline oxidase bienzyme system.<sup>67</sup> Enhancement of electron transfer between the enzyme and electrode and improvement of the biosensor sensitivity were observed. In another work, urease was trapped in chitosan– $\text{Fe}_3\text{O}_4$  nanocomposite for the creation of urea biosensor.<sup>68</sup> Authors stated that the composite material increased active surface area of the biosensor. Ultra-wide linear range (0.1 mM to 80 mM) of the urea biosensor based on urease/ $\text{Fe}_3\text{O}_4$ /chitosan was reported.<sup>69</sup> Glucose biosensor based on GOx immobilized on  $\text{Fe}_3\text{O}_4$  NPs/chitosan/graphene electrode also had wide linear range (up to 16 mM) with LOD of 16  $\mu\text{M}$ .<sup>70</sup>

### 3.6. Nanostructured titanium dioxide

Titanium nanotubes have large active surface due to huge number of nanopores and internal cavity. This, along with chemical stability, non-toxicity and charge transfer capability, makes  $\text{TiO}_2$  nanotubes a promising material for the enzyme immobilization in electrochemical biosensors.<sup>38</sup>  $\text{TiO}_2$  films are also perspective sensor components.<sup>71</sup>

For example, a composite material based on titanium nanotubes and polyaniline was used to immobilize GOx.<sup>72</sup> The biosensor was characterized by LOD of 0.5  $\mu\text{M}$  and a dynamic range of glucose determination 10–2500  $\mu\text{M}$ . However, the characteristics do not notably differ from those of similar glucose biosensors constructed without NMs.

The photoelectrochemical biosensor for the determination of hydrogen peroxide contained horseradish peroxidase and an array of  $\text{TiO}_2$  nanotubes covered with a polydopamine layer.<sup>39</sup> The biosensor was highly sensitive and selective, LOD was 0.7 nM, the detection range – 1 nM–50  $\mu\text{M}$ .

### 3.7. Zeolites and other nanosized aluminosilicates

Several types of nanosized aluminosilicates are known, in particular, zeolites, mesoporous silicon spheres, *etc.*<sup>73,74</sup> Zeolites, in turn, are divided into Beta, A, Y, LTA, silicalites, and other types (Fig. 4). The basic property of these nanoparticles is a highly ordered structure with a complex pore and canal system, based on a crystalline lattice of aluminum, silicon, and oxygen atoms (sometimes of silicon and oxygen only). This significantly increases the crystal surface area for the enzyme absorption.<sup>75</sup> Although aluminosilicates are inherently good adsorbents, they can be modified to further improve the enzyme immobilization.<sup>76</sup> Commonly, surface modification consists in the attachment of functional molecules containing carboxyl groups, amino groups, *etc.* The modification enhances the electrostatic bonds between the nanoparticle and the enzyme and allows for the formation of strong covalent bonds, for example, between carboxyl groups on the nanoparticle surface and amino groups of the enzyme. Additionally, different variants of zeolites with integrated metal ions can be used in electrochemical biosensors as the charge carriers.

At present, various types of zeolites were integrated in amperometric, potentiometric, and conductometric biosensors together with the enzymes GOx,<sup>78–80</sup> urease,<sup>81–84</sup> acetylcholinesterase,<sup>77</sup> butyrylcholinesterase,<sup>85</sup> creatinine deiminase,<sup>86</sup> glutamate oxidase,<sup>87</sup> *etc.* Zeolites in biosensors simplify the immobilization procedure and allow avoiding usage of toxic reagents, *e.g.*, glutaraldehyde. Additionally, better



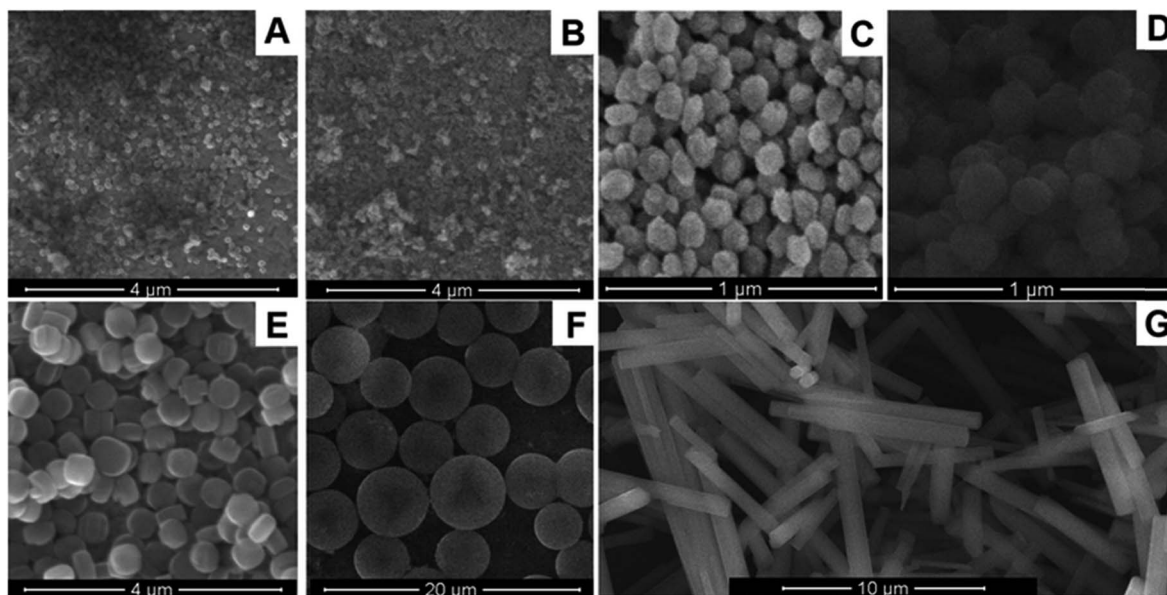


Fig. 4 Morphology of nanosized aluminosilicates: nanozeolite beta (A), nanozeolite L (B), 80 nm silicalite-1 (C), 160 nm silicalite-1 (D), 450 nm silicalite-1 (E), mesoporous silica spheres (F), zeolite L (G). Reproduced from ref. 77 Copyright 2015 Springer.

reproducibility of the biosensor preparation was shown. In some works, a 20–30% increase in the sensitivity of zeolite-based biosensors was observed.

### 3.8. Inorganic quantum dots

Quantum dots are semiconductor nanoscale crystals with unique optical properties.<sup>88</sup> They can consist of inorganic materials as well as of carbon or graphene. In the first place, quantum dots are used as fluorophores for generating light, so their application in electrochemical enzyme biosensors is rather unreasonable. Nevertheless, in some cases they were used.

A photoelectrochemical biosensor was proposed, which was based on glucose dehydrogenase immobilized on the electrode covered with quantum dots (ZnS and CdS) and multi-walled carbon nanotubes.<sup>89</sup> The biosensor was suitable for glucose determination in ampero- and photometric (at light irradiation) modes; the NMs, interacting with NADH formed in enzymatic reaction, generated the biosensor response. LOD was lower in case of the photoamperometric measurements than in usual amperometry (4  $\mu$ M and 6  $\mu$ M, respectively).

An amperometric biosensor for the determination of phenolic compounds contained tyrosinase, immobilized in a composite matrix of quantum dots (CdS) and chitosan.<sup>43</sup> The biosensor had a wide linear range of catechol detection (from 1 nM to 100  $\mu$ M) and low LOD (0.3 nM). According to the authors, it was due to the use of this highly porous, hydrophilic and biocompatible nanocomposite for the enzyme immobilization.

An amperometric biosensor proposed for the determination of cholesterol and its esters was based on the bi-enzyme system cholesterol esterase/cholesterol oxidase immobilized into a composite matrix of quantum dots (CdS) and chitosan.<sup>34</sup> The

authors believe that quantum dots mediated the electron transfer between the enzyme active center and the electrode. They also assumed an oriented enzyme immobilization near the quantum dot surface, which accelerated the charge transfer between the quantum dots and the enzymes as well as the participation of quantum dots in the electron transfer.<sup>90</sup>

The photoelectrochemical biosensor based on antibodies and horseradish peroxidase was proposed for the determination of carcinoembryonic antigen.<sup>91</sup> In the presence of the antigen, peroxidase catalyzed a multistage reaction near the electrode surface and the formation of CdS quantum dots on the surface of graphene oxide. When exposed to light, the dots generated a photocurrent, which was detected as the biosensor signal. This biosensor had a wide linear detection range from 2.5 ng mL<sup>-1</sup> to 50  $\mu$ g mL<sup>-1</sup> with LOD 0.72 ng mL<sup>-1</sup>.

### 3.9. Doped inorganic NMs

Properties of NMs can be tuned by doping.<sup>92</sup> Doping is a flexible way of NMs modification without significant change of their morphology, which leads to changes in electrical, optical, catalytic, and other properties.<sup>93</sup> Doped inorganic NMs can be used as sensor components separately or in combination with biomaterial. For example, recently described thiourea sensor is based on cobalt oxide codoped manganese oxide nanoparticles.<sup>94</sup> Ethanol<sup>95</sup> and acetone<sup>96</sup> sensors based on ternary-doped metal oxides are characterized by the extremely low LOD of 0.127 nM and 0.05 nM, respectively. Melamine sensor based on cadmium doped antimony oxide nanostructures had ultralow LOD (14 pM) as well.<sup>97</sup> Ultra-sensitive photoelectrochemical glucose biosensor has been constructed from the nitrogen-doped carbon sheets and titanium dioxide nanoparticles.<sup>98</sup> LOD was 13 nM, and linear range was shifted to low concentrations of glucose (0.05–10  $\mu$ M). Nitrogen-doped zinc

oxide thin films were used for construction of uric acid biosensor with a wide linear range (0.05–1.0 mM).<sup>99</sup>

### 3.10. Nanowires

Advances in nanotechnology make it possible to synthesize single nanowires and utilize them as sensitive elements of biosensors. In particular, nanowire field-effect transistors (FETs) attract significant attention.<sup>100</sup> As common FETs, they contain a gate, channel, source, drain, and the body, but the channel consists of a nanowire instead of a macrostructure. Silicon and silica nanowires are most widely used due to their high compatibility with the standard fabrication technology.<sup>100</sup> The main advantage of the nanowire-based FETs is high sensitivity – properties of nanowire (*i.e.*, conductance) are easily changed by processes that take place on its surface, thus biosensors can generate signal even when very small amounts of target molecules are present in the sample. Another advantages are low cost and possibility of multiplexed sensing using several FET on a single platform.<sup>101</sup> On the other hand, problem of high background noise arises.<sup>102</sup> Thus, special signal processing algorithms should be often used to split noise and useful signal.<sup>103</sup> Antibodies are often used as bioreceptors in such nanowire-based biosensors,<sup>104</sup> but several enzymes were also tested. For example, GOx was immobilized on the surface of FET based on  $\text{In}_2\text{O}_3$  nanoribbons.<sup>105</sup> Low LOD of 10 nM glucose was achieved, but storage stability was rather poor – more than 50% of sensitivity was lost after 2 weeks.

### 3.11. Nanorods

Nanorods are objects with length about 3–5 times larger than width. They are typically synthesized by direct chemical synthesis, which is not so convenient for biosensor applications as direct electrochemical synthesis on the transducer surface. Properties of nanorods are close to those of nanoparticles, and thus nanorods are applied in electrochemical biosensors mostly to improve electron transport and electrode surface area, but it should be noted that  $\text{ZnO}$  nanorods have semiconductor properties. Most commonly used nanorods are based on  $\text{ZnO}$

and gold.<sup>106</sup> Few electrochemical biosensors based on enzymes and nanorods were recently described. For example, galactose oxidase was immobilized on  $\text{ZnO}$  nanorods for the creation of galactose biosensor.<sup>107</sup> An interesting feature of the biosensor was linear range shifted towards high concentration of the target molecule (10–200 mM). The biosensor was selective against electroactive substances and did not change sensitivity during 4 weeks. In another work,  $\text{ZnO}$  nanorod arrays were used for GOx immobilization.<sup>108</sup> However, analytical characteristics of the biosensor (sensitivity, selectivity, linear range) were not significantly different from similar amperometric biosensors without nanorods.

## 4. Use of organic nanomaterials in enzyme-based biosensors

Organic NMs represented by CNTs,<sup>109</sup> graphene,<sup>110</sup> fullerenes,<sup>111</sup> calixarenes,<sup>112</sup> organic quantum dots, *etc.*, are widely used in the development of electrochemical biosensors due to their properties, enhancing electrochemical signal (Table 3). Additionally, organic NMs often have high biocompatibility, although it is generally worse than that of inorganic NMs.<sup>6</sup> The molecules with aromatic groups can be non-covalently bonded to the surface of graphene and CNTs *via* strong  $\pi$ – $\pi$  interactions. The hydrophobic molecules can also interact with the hydrophobic surface of organic NMs. However, this also may cause fouling, which is a significant problem for biological applications of graphene- or CNT-based biosensors.

### 4.1. Carbon nanotubes

CNT is a graphene sheet rolled up into a tube, which is characterized by high electrical conductivity, mechanical strength, and large surface area. The CNTs compatibility with other NMs and electrode materials is also important for electrochemical biosensors.<sup>13</sup> In the first place, conductive properties of CNTs are significant, because they enhance the enzyme-electrode charge transfer and, accordingly, sensitivity and response time of the biosensor. CNTs are classified as single- and multi-

Table 3 Examples of electrochemical biosensors based on enzymes and organic NMs<sup>a</sup>

Sensitive element	Analyte	Method of detection	Limit of detection	Sample	Ref.
GOx/CNT/mucin	Glucose	CA	3 $\mu\text{M}$	Human blood plasma	113
Horseradish peroxidase/CNT	Hydrogen peroxide	CV	22 nM	—	114
Urease/MWCNT	Urea	CA	30 $\mu\text{M}$	Blood plasma	115
Lysine oxidase/MWCNT/ $\text{SnO}_2$ /graphene/chitosan	Lysine	CA	0.15 $\mu\text{M}$	Dietary supplements	116
Laccase/graphene quantum dots	Epinephrine	CV	83 nM	Medicinal drug	117
Tyrosinase/graphene oxide	Phenolic compounds	CA	30 nM	Tap water	118
Soybean peroxidase/reduced graphene oxide	Hydrogen peroxide	CA	50 nM	Solution for contact lenses	119
GOx/reduced graphene oxide/ $\text{Fe}_3\text{O}_4$	Glucose	SWV, CA	—	—	120
Urease/fullerene $\text{C}_{60}$ /poly( <i>n</i> -butyl acrylate)	Urea	Potentiometry	42 $\mu\text{M}$	Urea	121

<sup>a</sup> SWV – square wave voltammetry; CA – chronoamperometry.



walled (SWCNT and MWCNT, respectively), depending on the number of graphene sheets rolled up into a tube. In biosensors, multi-walled CNTs are mostly used.

However, freshly synthesized CNTs have poor solubility in water, thus, it is difficult to bring them together with the aqueous solutions of enzymes. To improve solubility and biocompatibility, CNTs are functionalized with carboxylic or amino groups, or used in combination with other materials such as polymers or nanoparticles of metals.<sup>2</sup> The functionalized CNTs do not lose their initial high electrical conductivity and mechanical stability but can form suspensions in aqueous solutions and interact with enzymes *via* functional groups. This enables the development of CNT-based highly sensitive electrochemical biosensors.

CNTs are one of the most common NMs used in electrochemical enzyme-based biosensors. Numerous amperometric biosensors based on GOx and CNTs were described. For example, there is a biosensor, in which GOx was immobilized by cross-linking with glutaraldehyde, mucin and CNTs. It was shown that without CNTs, the biosensor was less sensitive and the analysis time was longer.<sup>113</sup> In,<sup>122</sup> MWCNTs modified with amino groups were applied when immobilizing GOx by cross-linking with glutaraldehyde; it resulted in a wider linear range of glucose determination and a higher biosensor sensitivity. In,<sup>123</sup> the biosensor based on GOx and polyaniline-modified MWCNTs was proposed; in ref. 124 GOx, SWCNTs and thermally expanded graphite were used.

A biosensor based on horseradish peroxidase and CNTs was characterized by the linear range of determination of hydrogen peroxide in low concentrations – from 0.1  $\mu$ M to 120  $\mu$ M.<sup>114</sup> The enzyme was modified with 4-aminothiophenol and immobilized by electropolymerization in CNT/polyaniline matrix (Fig. 5). LOD was 22 nM. Such biosensor can be adapted for

highly sensitive detection of other target molecules by incorporation of the  $\text{H}_2\text{O}_2$ -producing enzymes.

Other enzymes were also used together with CNTs in biosensors. The urea biosensor contained MWCNTs, conducting polymer poly(*o*-toluidine) and urease.<sup>115</sup> It had a wide range of urea determination – from 0.1 to 11 mM, which almost completely covered the possible urea concentrations in blood samples, but LOD was rather high (30  $\mu$ M). CNTs were also used to create the biosensors based on laccase,<sup>125</sup> peroxidase from zucchini (*Cucurbita pepo*),<sup>126</sup> lysine oxidase,<sup>116</sup> and others.

#### 4.2. Carbon quantum dots

Carbon quantum dots, or simply carbon dots, are nanosized carbon structures.<sup>127</sup> They are usually a few nanometers in size, chemically inert, suitable for various surface modifications, biocompatible, and cheap. Their greatest advantage is photoluminescent properties (not important for electrochemical sensing, though). Numerous optical (primarily fluorescent) biosensors with carbon dots have been described, however they are beyond the scope of this review.<sup>128–130</sup> We found only one electrochemical enzyme-based biosensor with carbon quantum dots. It was a horseradish peroxidase-based amperometric biosensor for hydrogen peroxide determination, which used carbon dots (2.8  $\pm$  0.5 nm) deposited on the surface of glassy carbon electrode.<sup>131</sup> The dots had amino acids on their surface and served as a matrix for the enzyme immobilization. The biosensor was highly sensitive, with LOD of 1.8 nM and a linear range of 5–590 nM.

Furthermore, the sensor based on carbon dots modified by magnetite particles was able to detect NADH in the range of 0.2–5  $\mu$ M.<sup>132</sup> Thus, these nanoparticles may be useful in electrochemical biosensors based on enzymes, which produce or use NADH.

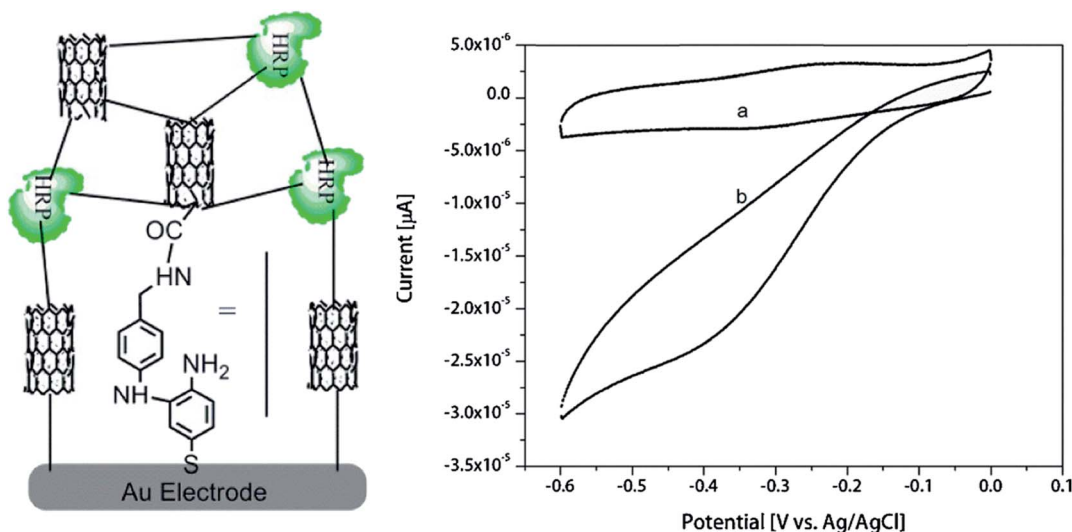


Fig. 5 Schematics of the hydrogen peroxide biosensor based on oligoaniline-cross-linked HRP/CNT composite and cyclic voltammograms of the biosensor obtained in the absence of  $\text{H}_2\text{O}_2$  (a) and in the presence of 5  $\mu$ M  $\text{H}_2\text{O}_2$  (b). Reprinted from *Enzyme and Microbial Technology*, 113, K. M. Kafi, M. Naqshabandi, M. M. Yusoff and M. J. Crossley, Improved peroxide biosensor based on Horseradish Peroxidase/Carbon Nanotube on a thiol-modified gold electrode, 67–74, Copyright (2017), with permission from Elsevier.<sup>114</sup>



### 4.3. Graphene quantum dots

Graphene quantum dots are nanosized graphene sheets similar to other quantum dots by their properties (biocompatibility, low toxicity, photostability, excellent fluorescence, high surface area). They are rarely used in conventional electrochemical biosensors, however an amperometric biosensor was developed for the determination of epinephrine in pharmaceuticals based on laccase immobilized with graphene quantum dots on the surface of a glassy carbon electrode.<sup>117</sup> The biosensor was characterized by a linear range of 1–120  $\mu$ M and a LOD of 83 nM. High selectivity was demonstrated, no impact of interfering substances (ascorbic and uric acids, cysteine, glutathione, and tryptophan) on the biosensor response was revealed. In another work laccase was immobilized on graphene quantum dots and molybdenum disulphide ( $\text{MoS}_2$ ) nanoflakes for the creation of the amperometric biosensor for polyphenol detection.<sup>133</sup> Synergetic effect between the two NMs was found, and nanocomposite matrix was favorable for the enzyme immobilization. Graphene quantum dots were used for GOx adsorption in glucose biosensors.<sup>134,135</sup> Direct electron transfer was observed, and the biosensors had better analytical characteristics than similar biosensors without quantum dots. Porosity of the NM and presence of hydrophilic and hydrophobic sites favored the GOx adsorption.

### 4.4. Graphene and its derivatives

Graphene is a one-atom thick sheet of carbon atoms arranged in a honeycomb-like structure. It is characterized by large surface area, excellent electrical and thermal conductivity, high mechanical stiffness.<sup>136</sup> Most of these parameters significantly exceed those of CNTs.<sup>137</sup>

Due to the large surface area of graphene, it is an effective substrate for the enzyme immobilization. The direct electron transfer between the enzyme and electrode is also enhanced because of high conductivity of graphene.<sup>138</sup> However, like CNTs, graphene is practically insoluble in water and many other solvents. To improve the hydrophilicity, additional nitrogen atoms are introduced into graphene structure, or graphene oxide (GO) is used, which relatively easily forms stable dispersions in an aqueous medium.<sup>139</sup> On the other hand, additional groups notably weaken conducting properties of graphene; therefore, GO is further reduced to rGO to decrease the number of oxygen-containing groups and achieve a balance between electric conductivity and solubility.

Graphene electrodes can be created either by direct printing of graphene ink or by printing a sacrificial polymer pattern followed by the graphene deposition.<sup>140,141</sup> On the other hand, graphene electrodes can be produced from carbon-based polymers (*i.e.*, polyimide) by  $\text{CO}_2$  laser irradiation.<sup>142</sup> In both cases the electrodes of relatively complex pattern (*e.g.*, interdigitated) can be easily obtained in large quantities suitable for the creation of amperometric, impedimetric or other types of biosensors. Although the specialized materials printer as well as  $\text{CO}_2$  laser cost tens of thousands of USD, they assure the manufacture of hundreds of uniform

electrodes per hour. Furthermore, raw materials for the process are cheap, and the electrode design can be modified quickly and conveniently in computer aided design software. Thus, graphene electrodes are promising for mass production and have clear advantages over the electrodes produced by traditional methods and subsequently modified with graphene. However, such electrodes are rarely utilized in enzyme-based biosensors; recent examples include diamine oxidase-based biosensor for the detection of biogenic amines (*e.g.*, histamine),<sup>143</sup> GOx-based glucose biosensor,<sup>144</sup> and phosphotriesterase-based biosensor for the detection of organophosphate pesticides.<sup>25</sup>

Still, although the graphene electrode itself is porous, its surface area can be further increased by creation of the conductive porous graphene/polymer composites as well as other porous graphene structures.<sup>145</sup>

An amperometric biosensor based on tyrosinase and GO for the determination of phenolic compounds is described in.<sup>118</sup> First, the glassy carbon electrode was modified with GO; afterwards glutaraldehyde was linked to free hydroxyl groups. Another end of glutaraldehyde formed covalent bonds with tyrosinase. A linear range of catechol determination was 50 nM to 50  $\mu$ M, LOD – 30 nM.

A biosensor based on acetylcholinesterase and a field-effect transistor modified with reduced GO was proposed.<sup>146</sup> It was used to determine the acetylcholinesterase activity and the concentration of the enzyme inhibitors donepezil and rivastigmine (drugs).

A biosensor based on soybean peroxidase and rGO was proposed for determination of hydrogen peroxide.<sup>119</sup> Usage of the NM made it possible to decrease the working potential to –0.09 V *vs.* Ag/AgCl reference electrode and to obtain LOD of 50 nM. The presence of interfering substances (ascorbic and uric acids, dopamine) did not affect the results of hydrogen peroxide determination.

In most works, single-enzyme biosensors are described. However, co-immobilization of several enzymes is also possible. For example, a bienzyme biosensor for the triglyceride and glycerol determination was proposed.<sup>147</sup> Lipase and glycerol dehydrogenase were co-immobilized on the surface of rGO modified with a mediator toluidine blue (Fig. 6). Lipase split triglycerides to glycerol and fatty acids, and then glycerol dehydrogenase oxidized glycerol with subsequent reduction of the mediator. The mediator was oxidized on the electrode surface. The biosensor demonstrated high selectivity, rapid response (12 s) and retained 90% of the initial sensitivity after 11 week. The triglyceride content in human blood serum was successfully analyzed.

A nanocomposite consisting of rGO and 50 nm  $\text{Fe}_3\text{O}_4$  nanoparticles was used for GOx adsorption in glucose biosensor.<sup>120</sup> The authors showed that the application of the nanocomposite allowed 4-fold improvement of conductivity of the electrode surface. The linear range of glucose determination was 0.5–10 mM. At a working potential –0.4 V *vs.* Ag/AgCl reference electrode the biosensor was not sensitive to dopamine, ascorbic and uric acids.



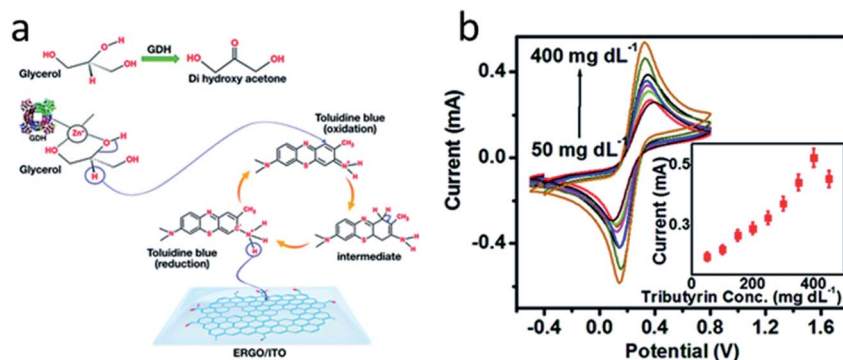


Fig. 6 (a) Chemical reactions that are the basis for the glycerol biosensor operation. Glycerol dehydrogenase (GDH), toluidine blue and electrochemically reduced graphene oxide (ERGO) are deposited on indium-tin oxide (ITO) electrode. Second enzyme (lipase) is not shown. (b) Response studies of the biosensor to varying concentrations of triglyceride (tributyrin). Inset: corresponding calibration curve. Reproduced from ref. 147 with permission from The Royal Society of Chemistry.

#### 4.5. Fullerenes

Fullerenes are closed spherical molecules with a pentagonal honeycomb structure made of carbon atoms. Due to high conductivity and large area of the hydrophobic surface on which the organic molecules could be adsorbed, fullerenes are promising for use in electrochemical biosensors as adsorbents and mediators to enhance the transport of electrons between an enzyme and an electrode.<sup>148,149</sup> Fullerenes are designated by the number of carbon atoms in the molecule, for example, C<sub>60</sub> – fullerene composed of 60 carbon atoms. The most commonly used fullerenes are C<sub>60</sub> and C<sub>70</sub>.

Fullerenes are not as common in electrochemical enzyme biosensors as CNTs and graphene derivatives, despite their high similarity. Fullerenes C<sub>60</sub> and C<sub>70</sub> were used as carriers for ascorbate oxidase in the biosensor system for the determination of ascorbic acid and phenols.<sup>150</sup> It turned out that much more enzyme molecules are immobilized on the surface of fullerenes than on SWCNTs and MWCNTs. Furthermore, fullerene C<sub>60</sub> was used as a urease carrier in the potentiometric biosensor for the urea determination.<sup>121</sup> The fullerene-urease conjugate was captured in a polymeric membrane, which provided excellent stability of immobilized urease, so the biosensor responses decreased by 5% after 140 days of dry storage at +4 °C.

The examples of other fullerene biosensors are the laccase-based biosensor for the determination of polyphenols in wine,<sup>149</sup> the glutathione reductase-based biosensor for the glutathione determination,<sup>151</sup> and a number of GOx-based biosensors for glucose determination in real samples.<sup>152,153</sup>

Furthermore, a glucose biosensor based on glucose dehydrogenase and AuNPs covered with C<sub>70</sub> fullerene was described.<sup>154</sup> This biosensor utilized multistep electron transfer: first the enzyme oxidized glucose and reduced NAD<sup>+</sup>, then NADH was reduced on the surface of the fullerene, the latter transferred electrons to AuNPs and then to the electrode (Fig. 7). The biosensor operated at relatively high working potential (+0.7 V), thus the negatively charged Nafion® membrane was placed over the enzyme membrane to repel interfering anions

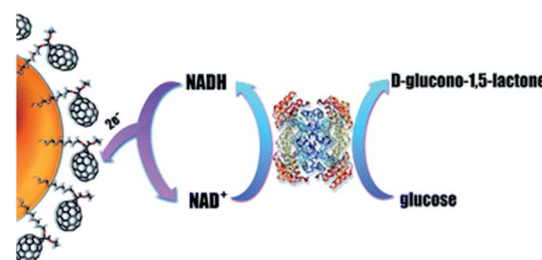


Fig. 7 Working principle of the glucose biosensor based on glucose dehydrogenase, fullerene C<sub>70</sub>, and AuNPs. Electrons from glucose are transferred to NAD<sup>+</sup>, fullerene, AuNPs, and finally to the working electrode. Reproduced from ref. 154 – published by The Royal Society of Chemistry.

(i.e., ascorbic and uric acids). The biosensor appeared to be highly selective.

Catalytic properties of fullerenes are poorly investigated. Nevertheless, it was shown that fullerene C<sub>60</sub> catalyzes oxidation of nandrolone (steroid hormone),<sup>155</sup> bisphenol A,<sup>156</sup> dopamine and ascorbic acid.<sup>157</sup>

#### 4.6. Calixarenes

Calixarenes are the cup-shaped chemical compounds consisting of several cyclic phenolic oligomers. Different variants of calixarene molecules can be synthesized and usually used as selective binding agents in sensors and chromatography columns. However, sometimes calixarenes and their derivatives are used as matrices for the enzyme immobilization.<sup>158,159</sup>

Effective GOx immobilization on a calixarene/AuNPs modified electrode was achieved.<sup>112</sup> Conductive polymer poly(2-(2-octyldodecyl)-4,7-di(selenoph-2-yl)-2H-benzo[*d*][1,2,3]triazole) was deposited on the electrode to improve conductance, then calixarene/AuNP suspension was drop-casted and calixarene formed thiol bonds with AuNPs (Fig. 8). Finally, GOx was covalently attached to the calixarene by *N*-(3-dimethylaminopropyl)-*N*-ethylcarbodiimide hydrochloride (EDC)/N-

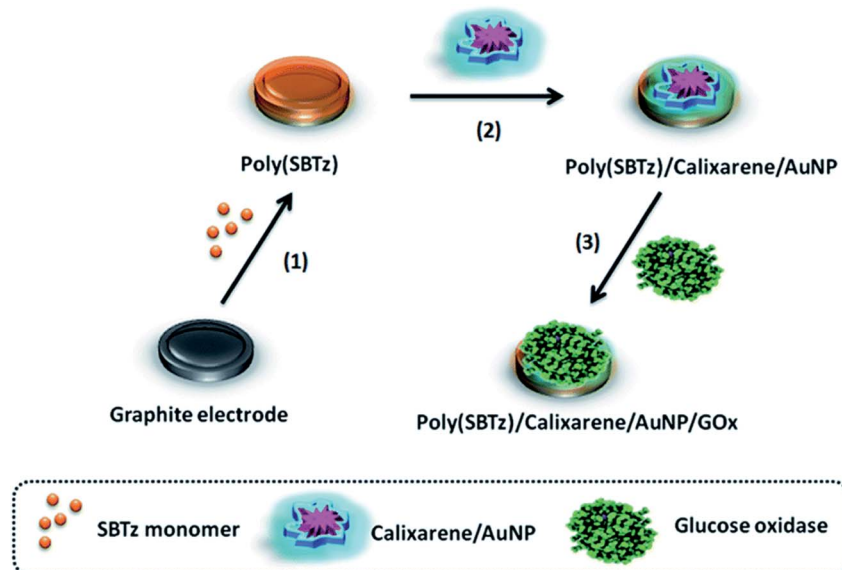


Fig. 8 Preparation of the glucose biosensor based on conductive polymer poly(2-(2-octyldodecyl)-4,7-di(selenoph-2-yl)-2H-benzo[d][1,2,3]triazole) (poly(SBTz)), calixarene, AuNPs and GOx. Graphite electrode is modified with conductive polymer, calixarene, and AuNPs followed by GOx immobilization. Reproduced from ref. 112 with permission from The Royal Society of Chemistry.

hydroxysuccinimide (NHS) crosslinking agents. The biosensor operated at the working potential of  $-0.7$  V vs. Ag wire and was successfully used to determine glucose in beverages.

A series of biosensors using calixarenes were developed for glucose determination in beverages;<sup>160</sup> calixarenes can be also promising in the conductometric enzyme biosensors for ammonia detection.<sup>161</sup>

#### 4.7. Conducting polymers

Conducting (or conductive) polymers are large organic molecules that are electrically conductive. Examples of conducting polymers include poly(acetylene), poly(thiophene), poly(pyrrole), and poly(aniline).<sup>162</sup> They are widely used in electrochemical biosensors to enhance electron transfer between the enzyme and the electrode and to improve conditions of the enzyme immobilization.<sup>163</sup> Thus, conducting polymers are usually used in amperometric biosensors based on oxidoreductase enzymes, where charge transfer plays especially important role. Generally, biosensors based on conducting polymers are characterized by higher sensitivity than similar biosensors without polymers due to greatly increased electron transfer between the enzyme active center and the electrode surface.<sup>164</sup> Another reason for popularity of the conducting polymers in biosensors is the ease of their synthesis, which is usually done electrochemically directly on the electrode surface. Entrapment of enzymes can occur during synthesis, which simplifies the biosensor preparation. Examples of biosensors based on conducting polymers include glucose biosensor based on GOx,<sup>165–167</sup> H<sub>2</sub>O<sub>2</sub> biosensor based on horseradish peroxidase,<sup>165</sup> urea biosensor based on urease,<sup>168</sup> and cholesterol biosensor based on cholesterol oxidase.<sup>169</sup>

## 5. Application of composite nanomaterials in electrochemical biosensors

The combination of several types of NMs in a single biosensor is gaining popularity. Composite nanoparticles containing several metal oxides can be prepared.<sup>170,171</sup> Furthermore, metal-based NMs can be combined with CNTs,<sup>172,173</sup> graphene, rGO,<sup>174</sup> polymers,<sup>175</sup> etc., and used to immobilize enzymes. This can lead to a synergistic effect of NMs on the characteristics of biosensors. In more detail, an application of hybrid composite materials in biosensors was reviewed in.<sup>176</sup>

Most often GOx is used in combination with several NMs. For example, a glucose biosensor contained GOx immobilized on a gold electrode modified with rGO and platinum–gold nanoparticles.<sup>177</sup> A LOD (1  $\mu$ M) was not outstanding, but the linear range was very wide (0.01–8 mM). The biosensor showed good storage stability – after one month its sensitivity decreased by only 18%. The working potential was relatively high (+0.6 V) despite the application of NMs.

In another work GOx was immobilized along with CNTs and PtNPs; the hydrogen peroxide reduction was observed at the working potential  $-0.1$  V.<sup>35</sup> The biosensor was characterized by a very fast response (2 s), a LOD of 6  $\mu$ M, and a linear range of 50  $\mu$ M to 5 mM. In the similar work, glutamate oxidase was immobilized together with carbon nanotubes and AuNPs; a low potential (+0.135 V) was used for hydrogen peroxide oxidation.<sup>37</sup> The biosensor had a fast response (2 s), a LOD of 1.6  $\mu$ M, and a linear range of 5–500  $\mu$ M.

A glucose biosensor was proposed based on GOx and nanocomposite consisting of nanosheets of rGO and AgNPs.<sup>178</sup> The nanocomposite had high biocompatibility and conductivity,



and the biosensor was characterized by excellent analytical parameters – a LOD of 25 nM, a high sensitivity of  $15.32 \text{ mA M}^{-1} \text{ cm}^{-2}$  and a linear range from 150 nM to 10 mM.

Another glucose biosensor was based on field-effect transistor (FET) and GOx, immobilized with graphene, modified with flower-shaped Pd nanostructures (Fig. 9).<sup>179</sup> The biosensor had relatively complex structure: graphene was located in the bottom layer and functioned as a working electrode, then Pd nanoflowers were electrodeposited and patterned with gold, next Nafion®/rGO membrane was deposited by spin coating, and finally GOx/GO dispersion was drop-casted. Thus, GOx was entrapped in a matrix formed by GO and rGO. The biosensor had a low LOD (1 nM) and was insensitive to common interferents (uric and ascorbic acids).

A biosensor for catechol determination has been recently described which was based on tyrosinase immobilized together

with MWCNTs and gold nanowires.<sup>180</sup> Due to the synergetic effect of the two nanostructures, it was possible to achieve a low LOD (0.027  $\mu\text{M}$ ).

An ultrasensitive biosensor for tyrosine determination was based on tyrosine hydroxylase immobilized in a composite material consisting of chitosan, nanoparticles of platinum/palladium alloy, graphene and MWCNTs.<sup>181</sup> The biosensor was highly selective and had a very low LOD (9 pM).

In another work,<sup>182</sup> a printed carbon electrode was modified by a composite membrane containing CNTs, nanosized zirconium oxide, Prussian blue, and a polymer Nafion® membrane. Additionally, acetylcholinesterase was immobilized on the surface of magnetic nanoparticles ( $\text{Fe}_3\text{O}_4/\text{Au}$ ) through covalent bonds Au-S. Under the action of an external magnetic field, the nanoparticles with acetylcholinesterase came into a contact with

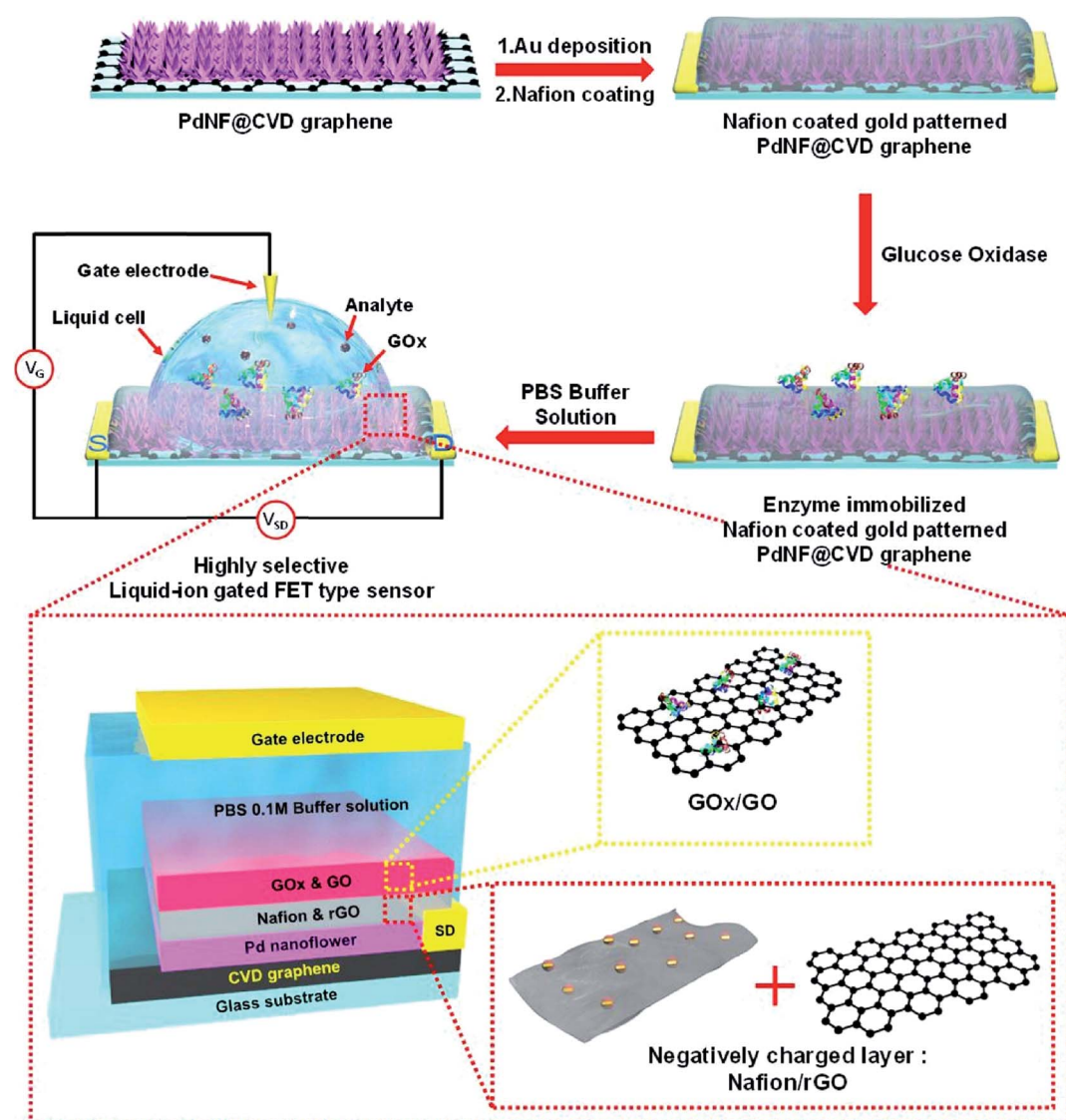


Fig. 9 Schematic diagram of the fabrication of FET glucose biosensor (top) and structure of the biosensor sensitive element (bottom). For the biosensor fabrication, Pd nanoflowers were electrodeposited and patterned with gold, then Nafion®/rGO membrane was deposited by spin coating, and finally GOx/GO dispersion was drop-casted. Reprinted from *Sensors and Actuators B: Chemical*, 264, D. H. Shin, W. Kim, J. Jun, J. S. Lee, J. H. Kim and J. Jang, Highly selective FET-type glucose sensor based on shape-controlled palladium nanoflower-decorated graphene, 216–223, Copyright (2018), with permission from Elsevier.<sup>179</sup>



the modified electrode to form a biosensor. After analysis, the magnetic field was switched off, the nanoparticles with the enzyme were washed out, and the modified electrode was reused to create new biosensors. In such a way, a high sensitivity to the organophosphorus pesticide dimethoate was achieved. LOD was  $5.6 \times 10^{-4}$  ng mL $^{-1}$ , the linear range  $1.0 \times 10^{-3}$  to 10 ng mL $^{-1}$ .

## 6. Problems associated with the application of nanomaterials in enzyme-based biosensors

From the above data it can be concluded that the application of NMs in enzyme-based biosensors is very attractive for the researchers and this field is rapidly expanding without any problems. However, a few negative tendencies in the NMs application should be noted.

One issue is that instead of a comprehensive evaluation of benefits of one certain NM the researchers often make a quick study and move to another kind of NMs and their combinations. This is partially explained by the fact that it is much more difficult to publish a second article describing the biosensor with the same NM, since the work will be considered less novel. As a result of such rush for novelty, a large number of papers about enzyme/NM-based biosensors are published each month, but it is very difficult to analyze them since each research group tries to use a unique NM only to distinguish their work from others. Indeed, almost any newly described biosensor contains one or several NMs, and a combination of NMs is one of the easiest ways to stand out from dozens of similar publications. Such approach often allows publication of the manuscript even if no clear advantage over biosensors without NMs is presented.

Furthermore, some authors report unbelievably good results (*i.e.*, extremely low LOD of a biosensor) attributing them to the influence of NMs. This allows researchers to claim that they have created the most sensitive or otherwise great biosensor and thus get published in the top-rated journals. In our opinion, it would be quite difficult, if even possible, to reproduce such results. Although we cannot estimate the exact amount of papers with partially or completely fake results, we consider that the amount is sufficiently high to raise a concern about the repeatability of experiments, especially in case of reporting LOD below 10 nM, or extremely good stability over several months. Meanwhile, the researchers remain relatively safe, since nobody will repeat their work because replication studies are usually not funded and cannot be published due to the lack of novelty.<sup>183</sup> Furthermore, even if somebody replicates a work (unsuccessfully), it is easy to explain the different results by improper synthesis of NMs, variance in methodology, materials, equipment, *etc.* Unfortunately, such action makes it difficult to other researchers to publish real, but worse results. The problem of replication is common for different research areas, and hopefully some solutions will be found in future.<sup>184</sup>

## 7. Conclusions

The development of enzyme-based electrochemical biosensors based on nanomaterials is an important direction of biosensor

research and it will remain an important field in the nearest future. Today, the modified biosensors are proposed for many fields, including the food industry, clinical diagnosis, biomedicine, environmental monitoring. The main effects of NMs application in electrochemical enzyme-based biosensors can be divided into three groups: (1) enhancement of the charge transfer between the enzyme and the electrode (up to direct electron transfer); (2) improvement of conditions of enzyme immobilization and stability; (3) catalysis of electrochemical reactions. Although there is a large variety of NMs that differ in chemical structure, properties, and morphology, positive effects of NMs in biosensors are caused mostly by the three factors: large surface area-to-volume ratio, high conductance, and excellent biocompatibility. In few cases (PtNPs and PdNPs), catalytic properties of NMs are also important. Application of NMs is also favored by their simple synthesis, which is often performed electrochemically directly on the electrode surface.

Wide perspectives are opening for biosensors based on nanocomposites and newly discovered nanostructures. Utilization of nanomaterials with specifically tailored properties (*i.e.*, designed receptor sites) is also growing. Application of NMs is expected to improve selectivity, sensitivity, storage stability, and other analytical characteristics of electrochemical biosensors. Such improvements will make biosensors more robust and increase their practical application.

## 8. Glossary

AgNP	Silver nanoparticle
AuE	Gold electrode
AuNP	Gold nanoparticle
CA	Chronoamperometry
CNT	Carbon nanotube
CV	Cyclic voltammetry
FET	Field-effect transistor
GCE	Glassy carbon electrode
GO	Graphene oxide
GOx	Glucose oxidase
ITO	Indium tin oxide
LOD	Limit of detection
MWCNT	Multi-walled carbon nanotube
NAD <sup>+</sup>	Oxidized nicotinamide adenine dinucleotide
NADH	Reduced nicotinamide adenine dinucleotide
NM	Nanomaterial
NP	Nanoparticle
NT	Nanotube
PdNP	Palladium nanoparticle
PtNP	Platinum nanoparticle
rGO	Reduced graphene oxide
SPE	Screen-printed electrode
SWV	Square wave voltammetry
SWCNT	Single-walled carbon nanotube
TNM	<i>tert</i> -Nonyl mercaptan
QDs	Quantum dots



## Conflicts of interest

There are no conflicts to declare.

## Acknowledgements

This work was supported by the State Budget Program “Support for the Development of Priority Areas of Scientific Research” (Code: 6541230) through a program of National Academy of Sciences of Ukraine “Smart sensor devices of a new generation based on modern materials and technologies”.

## References

- 1 D. R. Thevenot, K. Tóth, R. A. Durst and G. S. Wilson, *Pure Appl. Chem.*, 1999, **71**, 2333–2348.
- 2 Y. Zeng, Z. Zhu, D. Du and Y. Lin, *J. Electroanal. Chem.*, 2016, **781**, 147–154.
- 3 W. Jin and G. Maduraiveeran, *J. Anal. Sci. Technol.*, 2018, **9**, 18.
- 4 M. N. Arshad, T. A. Sheikh, M. M. Rahman, A. M. Asiri, H. M. Marwani and M. R. Awual, *J. Organomet. Chem.*, 2017, **827**, 49–55.
- 5 M. M. Hussain, M. M. Rahman, M. N. Arshad and A. M. Asiri, *ACS Omega*, 2017, **2**, 420–431.
- 6 S. Kurbanoglu, S. A. Ozkan and A. Merkoçi, *Biosens. Bioelectron.*, 2017, **89**, 886–898.
- 7 M. M. Rahman and A. M. Asiri, *RSC Adv.*, 2015, **5**, 63252–63263.
- 8 M. R. Awual, M. Khraisheh, N. H. Alharthi, M. Luqman, A. Islam, M. Rezaul Karim, M. M. Rahman and M. A. Khaleque, *Chem. Eng. J.*, 2018, **343**, 118–127.
- 9 M. R. Awual, N. H. Alharthi, Y. Okamoto, M. R. Karim, M. E. Halim, M. M. Hasan, M. M. Rahman, M. M. Islam, M. A. Khaleque and M. C. Sheikh, *Chem. Eng. J.*, 2017, **320**, 427–435.
- 10 M. R. Awual, M. M. Hasan, G. E. Eldesoky, M. A. Khaleque, M. M. Rahman and M. Naushad, *Chem. Eng. J.*, 2016, **290**, 243–251.
- 11 M. R. Awual, N. H. Alharthi, M. M. Hasan, M. R. Karim, A. Islam, H. Znad, M. A. Hossain, M. E. Halim, M. M. Rahman and M. A. Khaleque, *Chem. Eng. J.*, 2017, **324**, 130–139.
- 12 M. R. Awual, A. M. Asiri, M. M. Rahman and N. H. Alharthi, *Chem. Eng. J.*, 2019, **363**, 64–72.
- 13 G. Maduraiveeran and W. Jin, *Trends Environ. Anal. Chem.*, 2017, **13**, 10–23.
- 14 M. M. Alam, M. A. Rashed, M. M. Rahman, M. M. Rahman, Y. Nagao and M. A. Hasnat, *RSC Adv.*, 2018, **8**, 8071–8079.
- 15 M. M. Hussain, A. M. Asiri, M. N. Arshad and M. M. Rahman, *New J. Chem.*, 2018, **42**, 1169–1180.
- 16 S. Nawaz, S. Khan, U. Farooq, M. S. Haider, N. M. Ranjha, A. Rasul, A. Nawaz, N. Arshad and R. Hameed, *Des. Monomers Polym.*, 2018, **21**, 18–32.
- 17 H. Li and D. Xu, *TrAC, Trends Anal. Chem.*, 2014, **61**, 67–73.
- 18 Y. Wang, K. Qu, L. Tang, Z. Li, E. Moore, X. Zeng, Y. Liu and J. Li, *TrAC, Trends Anal. Chem.*, 2014, **58**, 54–70.
- 19 V. V. Pokropivny and V. V. Skorokhod, *Mater. Sci. Eng., C*, 2007, **27**, 990–993.
- 20 M. M. Rahman, *Sens. Actuators, B*, 2018, **264**, 84–91.
- 21 A. M. Asiri, M. M. Hussain, M. N. Arshad and M. M. Rahman, *New J. Chem.*, 2018, **42**, 4465–4473.
- 22 M. M. Rahman, M. M. Alam, A. M. Asiri and M. R. Awual, *New J. Chem.*, 2017, **41**, 9159–9169.
- 23 A. Umar, M. M. Rahman, S. H. Kim and Y.-B. Hahn, *Chem. Commun.*, 2008, 166–168.
- 24 A. A. P. Khan, A. Khan, M. M. Rahman, A. M. Asiri and M. Oves, *Int. J. Biol. Macromol.*, 2017, **98**, 256–267.
- 25 J. A. Hondred, J. C. Breger, N. J. Alves, S. A. Trammell, S. A. Walper, I. L. Medintz and J. C. Claussen, *ACS Appl. Mater. Interfaces*, 2018, **10**, 11125–11134.
- 26 I. Rassas, M. Braiek, A. Bonhomme, F. Bessueille, G. Rafin, H. Majdoub and N. Jaffrezic-Renault, *Mater. Sci. Eng., C*, 2019, **95**, 152–159.
- 27 M. Badea, A. Curulli and G. Palleschi, *Biosens. Bioelectron.*, 2003, **18**, 689–698.
- 28 K. Kerman, M. Saito, E. Tamiya, S. Yamamura and Y. Takamura, *TrAC, Trends Anal. Chem.*, 2008, **27**, 585–592.
- 29 N. Li, P. Zhao and D. Astruc, *Angew. Chem., Int. Ed.*, 2014, **53**, 1756–1789.
- 30 R. G. Weiner and S. E. Skrabalak, *Angew. Chem., Int. Ed.*, 2015, **54**, 1181–1184.
- 31 K. D. Gilroy, A. Ruditskiy, H.-C. Peng, D. Qin and Y. Xia, *Chem. Rev.*, 2016, **116**, 10414–10472.
- 32 R. Sinha, M. Ganesana, S. Andreeescu and L. Stanciu, *Anal. Chim. Acta*, 2010, **661**, 195–199.
- 33 N. Chauhan and C. S. Pundir, *Electrochim. Acta*, 2012, **67**, 79–86.
- 34 H. Dhyani, M. A. Ali, S. P. Pal, S. Srivastava, P. R. Solanki, B. D. Malhotra and P. Sen, *RSC Adv.*, 2015, **5**, 45928–45934.
- 35 H. N. Choi, J. H. Han, J. A. Park, J. M. Lee and W.-Y. Lee, *Electroanalysis*, 2007, **19**, 1757–1763.
- 36 S. H. Lim, J. Wei, J. Lin, Q. Li and J. KuaYou, *Biosens. Bioelectron.*, 2005, **20**, 2341–2346.
- 37 B. Batra and C. S. Pundir, *Biosens. Bioelectron.*, 2013, **47**, 496–501.
- 38 F. Wu, J. Xu, Y. Tian, Z. Hu, L. Wang, Y. Xian and L. Jin, *Biosens. Bioelectron.*, 2008, **24**, 198–203.
- 39 J. Li, X. Li, Q. Zhao, Z. Jiang, M. Tadé, S. Wang and S. Liu, *Sens. Actuators, B*, 2018, **255**, 133–139.
- 40 F. W. P. Ribeiro, M. F. Barroso, S. Morais, S. Viswanathan, P. de Lima-Neto, A. N. Correia, M. B. P. P. Oliveira and C. Delerue-Matos, *Bioelectrochemistry*, 2014, **95**, 7–14.
- 41 M. A. Abrar, Y. Dong, P. K. Lee and W. S. Kim, *Sci. Rep.*, 2016, **6**, 30565.
- 42 T. Liu, M. Xu, H. Yin, S. Ai, X. Qu and S. Zong, *Microchim. Acta*, 2011, **175**, 129–135.
- 43 E. Han, Y. Yang, Z. He, J. Cai, X. Zhang and X. Dong, *Anal. Biochem.*, 2015, **486**, 102–106.
- 44 J. A. Hondred, J. C. Breger, N. T. Garland, E. Oh, K. Susumu, S. A. Walper, I. L. Medintz and J. C. Claussen, *Analyst*, 2017, **142**, 3261–3271.
- 45 G. A. Valencia, L. C. de Oliveira Vercik and A. Vercik, *J. Polym. Eng.*, 2014, **34**, 633–638.



46 C. Vaghela, M. Kulkarni, S. Haram, R. Aiyer and M. Karve, *Int. J. Biol. Macromol.*, 2018, **108**, 32–40.

47 Y. Zhou, M. Wang, H. Yin and S. Ai, *Microchim. Acta*, 2017, **184**, 3301–3308.

48 V. Pavlov, Y. Xiao and I. Willner, *Nano Lett.*, 2005, **5**, 649–653.

49 M. Taguchi, N. Schwalb, Y. Rong, D. C. Vanegas, N. Garland, M. Tan, H. Yamaguchi, J. C. Claussen and E. S. McLamore, *Analyst*, 2016, **141**, 3367–3378.

50 E. Lebègue, C. M. Anderson, J. E. Dick, L. J. Webb and A. J. Bard, *Langmuir*, 2015, **31**, 11734–11739.

51 Y. Li, C. Sella, F. Lemaître, M. Guille Collignon, L. Thouin and C. Amatore, *Electroanalysis*, 2013, **25**, 895–902.

52 B. Rismetov, T. A. Ivandini, E. Saepudin and Y. Einaga, *Diamond Relat. Mater.*, 2014, **48**, 88–95.

53 H. Olivia, B. V. Sarada, K. Honda and A. Fujishima, *Electrochim. Acta*, 2004, **49**, 2069–2076.

54 L. Wang, J. Li, Y. Pan, L. Min, Y. Zhang, X. Hu and Z. Yang, *Microchim. Acta*, 2017, **184**, 2357–2363.

55 S. B. Adelaju and S. Hussain, *Microchim. Acta*, 2016, **183**, 1341–1350.

56 F. N. Crespilho, R. M. Iost, S. A. Travain, O. N. Oliveira and V. Zucolotto, *Biosens. Bioelectron.*, 2009, **24**, 3073–3077.

57 T. Kavetskyy, O. Smutok, M. Gonchar, O. Demkiv, H. Klepach, Y. Kukhazh, O. Šauša, T. Petkova, V. Boev, V. Ilcheva, P. Petkov and A. L. Stepanov, *J. Appl. Polym. Sci.*, 2017, **134**, 45278.

58 J. Wang, X. Chen, K. Liao, G. Wang and M. Han, *Nanoscale Res. Lett.*, 2015, **10**, 311.

59 M. Barquero-Quirós and M. Arcos-Martínez, *Sensors*, 2016, **16**, 1588.

60 V. Guzsvány, J. Anojčić, E. Radulović, O. Vajdle, I. Stanković, D. Madarász, Z. Kónya and K. Kalcher, *Microchim. Acta*, 2017, **184**, 1987–1996.

61 Q. Zeng, J.-S. Cheng, X.-F. Liu, H.-T. Bai and J.-H. Jiang, *Biosens. Bioelectron.*, 2011, **26**, 3456–3463.

62 S. Bozkurt, B. Tosun, B. Sen, S. Akocak, A. Savk, M. F. Ebeoglugil and F. Sen, *Anal. Chim. Acta*, 2017, **989**, 88–94.

63 L. Gao, K. Fan and X. Yan, *Theranostics*, 2017, **7**, 3207–3227.

64 N. SanaEIFAR, M. Rabiee, M. Abdolrahim, M. Tahriri, D. Vashaee and L. Tayebi, *Anal. Biochem.*, 2017, **519**, 19–26.

65 C. He, M. Xie, F. Hong, X. Chai, H. Mi, X. Zhou, L. Fan, Q. Zhang, T. Ngai and J. Liu, *Electrochim. Acta*, 2016, **222**, 1709–1715.

66 N. Mohamad Nor, K. Abdul Razak and Z. Lockman, *Electrochim. Acta*, 2017, **248**, 160–168.

67 E. Ö. Bolat, G. A. Tiğ and Ş. Pekyardımcı, *J. Electroanal. Chem.*, 2017, **785**, 241–248.

68 M. W. Akram, M. F. Alam, H. N. Ji, A. Mahmood, T. Munir, M. Z. Iqbal, M. R. Saleem, N. Amin and A. G. Wu, *IOP Conf. Ser.: Mater. Sci. Eng.*, 2019, **474**, 012060.

69 A. Ali, M. S. AlSalhi, M. Atif, A. A. Ansari, M. Q. Israr, J. R. Sadaf, E. Ahmed, O. Nur and M. Willander, *J. Phys.: Conf. Ser.*, 2013, **414**, 012024.

70 W. Zhang, X. Li, R. Zou, H. Wu, H. Shi, S. Yu and Y. Liu, *Sci. Rep.*, 2015, **5**, 11129.

71 M. M. Rahman, V. G. Alfonso, F. Fabregat-Santiago, J. Bisquert, A. M. Asiri, A. A. Alshehri and H. A. Albar, *Microchim. Acta*, 2017, **184**, 2123–2129.

72 J. Zhu, X. Liu, X. Wang, X. Huo and R. Yan, *Sens. Actuators, B*, 2015, **221**, 450–457.

73 W.-H. Chen, S.-J. Huang, H.-H. Ko, A.-Y. Lo, H.-K. Lee, L.-L. Wu, C.-F. Cheng and S.-B. Liu, *Stud. Surf. Sci. Cat.*, 2005, **156**, 657–662.

74 S. Mintova, J.-P. Gilson and V. Valtchev, *Nanoscale*, 2013, **5**, 6693.

75 M. G. Valdés, A. I. Pérez-Cordoves and M. E. Díaz-García, *TrAC, Trends Anal. Chem.*, 2006, **25**, 24–30.

76 C. Ispas, I. Sokolov and S. Andreeescu, *Anal. Bioanal. Chem.*, 2009, **393**, 543–554.

77 I. Kucherenko, O. Soldatkin, B. O. Kasap, S. K. Kirdeciler, B. A. Kurc, N. Jaffrezic-Renault, A. Soldatkin, F. Lagarde and S. Dzyadevych, *Nanoscale Res. Lett.*, 2015, **10**, 209.

78 R. Nenkova, J. Wu, Y. Zhang and T. Godjevargova, *Anal. Biochem.*, 2013, **439**, 65–72.

79 O. O. Soldatkin, B. Ozansoy Kasap, B. Akata Kurc, A. P. Soldatkin, S. V. Dzyadevych and A. V. El'skaya, *Biopolym. Cell*, 2014, **30**, 291–298.

80 V. N. Pyeshkova, O. Y. Dudchenko, O. O. Soldatkin, I. S. Kucherenko, B. Ozansoy Kasap, B. Akata Kurc and S. V. Dzyadevych, *Biopolym. Cell*, 2014, **30**, 462–468.

81 M. Hamlaoui, K. Reybier, M. Marrakchi, N. Jaffrezic-Renault, C. Martelet, R. Kherrat and A. Walcarius, *Anal. Chim. Acta*, 2002, **466**, 39–45.

82 M. K. Shelyakina, O. O. Soldatkin, V. M. Arkhypova, B. O. Kasap, B. Akata and S. V. Dzyadevych, *Nanoscale Res. Lett.*, 2014, **9**, 124.

83 O. O. Soldatkin, I. S. Kucherenko, S. V. Marchenko, B. Ozansoy Kasap, B. Akata, A. P. Soldatkin and S. V. Dzyadevych, *Mater. Sci. Eng., C*, 2014, **42**, 155–160.

84 I. S. Kucherenko, O. O. Soldatkin, B. O. Kasap, S. Öztürk, B. Akata, A. P. Soldatkin and S. V. Dzyadevych, *Electroanalysis*, 2012, **24**, 1380–1385.

85 E. Soy, V. Arkhypova, O. Soldatkin, M. Shelyakina, S. Dzyadevych, J. Warzywoda, A. Sacco and B. Akata, *Mater. Sci. Eng., C*, 2012, **32**, 1835–1842.

86 B. Ozansoy Kasap, S. V. Marchenko, O. O. Soldatkin, S. V. Dzyadevych and B. Akata Kurc, *Nanoscale Res. Lett.*, 2017, **12**, 162.

87 O. V. Soldatkina, O. O. Soldatkin, B. O. Kasap, D. Y. Kucherenko, I. S. Kucherenko, B. A. Kurc and S. V. Dzyadevych, *Nanoscale Res. Lett.*, 2017, **12**, 260.

88 L. Cui, C. Li, B. Tang and C. Zhang, *Analyst*, 2018, **143**, 2469–2478.

89 B. Ertek and Y. Dilgin, *Bioelectrochemistry*, 2016, **112**, 138–144.

90 G. Zhiguo, Y. Shuping, L. Zaijun, S. Xiulan, W. Guangli, F. Yinjun and L. Junkang, *Electrochim. Acta*, 2011, **56**, 9162–9167.

91 X. Zeng, W. Tu, J. Li, J. Bao and Z. Dai, *ACS Appl. Mater. Interfaces*, 2014, **6**, 16197–16203.

92 T. C. Bharat, Shubham, S. Mondal, H. S. Gupta, P. K. Singh and A. K. Das, *Mater. Today: Proc.*, 2019, **11**, 767–775.



93 X. Chen, Y. Lou, S. Dayal, X. Qiu, R. Krolicki, C. Burda, C. Zhao and J. Becker, *J. Nanosci. Nanotechnol.*, 2005, **5**, 1408–1420.

94 M. M. Rahman, J. Ahmed and A. M. Asiri, *Biosens. Bioelectron.*, 2018, **99**, 586–592.

95 M. M. Rahman, M. M. Alam, A. M. Asiri and M. A. Islam, *RSC Adv.*, 2017, **7**, 22627–22639.

96 M. M. Rahman, M. M. Alam, A. M. Asiri and M. A. Islam, *Talanta*, 2017, **170**, 215–223.

97 M. M. Rahman and J. Ahmed, *Biosens. Bioelectron.*, 2018, **102**, 631–636.

98 R. Atchudan, N. Muthuchamy, T. N. J. I. Edison, S. Perumal, R. Vinodh, K. H. Park and Y. R. Lee, *Biosens. Bioelectron.*, 2019, **126**, 160–169.

99 K. Jindal, M. Tomar and V. Gupta, *Analyst*, 2013, **138**, 4353.

100 P. Ambhorkar, Z. Wang, H. Ko, S. Lee, K. Koo, K. Kim and D. Cho, *Micromachines*, 2018, **9**, 679.

101 A. Gao, X. Yang, J. Tong, L. Zhou, Y. Wang, J. Zhao, H. Mao and T. Li, *Biosens. Bioelectron.*, 2017, **91**, 482–488.

102 Y. Kutowyi, I. Zadorozhnyi, H. Hlukhova, V. Handziuk, M. Petrychuk, A. Ivanchuk and S. Vitusevich, *Nanotechnology*, 2018, **29**, 175202.

103 Y. Kutowyi, I. Zadorozhnyi, V. Handziuk, H. Hlukhova, N. Boichuk, M. Petrychuk and S. Vitusevich, *Phys. Status Solidi A*, 2019, **256**, 1800636.

104 M.-A. Doucey and S. Carrara, *Trends Biotechnol.*, 2019, **37**, 86–99.

105 Q. Liu, Y. Liu, F. Wu, X. Cao, Z. Li, M. Alharbi, A. N. Abbas, M. R. Amer and C. Zhou, *ACS Nano*, 2018, **12**, 1170–1178.

106 X. Huang, S. Neretina and M. A. El-Sayed, *Adv. Mater.*, 2009, **21**, 4880–4910.

107 K. Khun, Z. H. Ibupoto, O. Nur and M. Willander, *J. Sens.*, 2012, **2012**, 1–7.

108 N. S. Ridhuan, K. Abdul Razak and Z. Lockman, *Sci. Rep.*, 2018, **8**, 13722.

109 A. Battigelli, C. Ménard-Moyon, T. Da Ros, M. Prato and A. Bianco, *Adv. Drug Delivery Rev.*, 2013, **65**, 1899–1920.

110 Y. Shao, J. Wang, H. Wu, J. Liu, I. A. Aksay and Y. Lin, *Electroanalysis*, 2010, **22**, 1027–1036.

111 S. Pilehvar and K. De Wael, *Biosensors*, 2015, **5**, 712–735.

112 T. C. Gokoglan, S. Soylemez, M. Kesik, H. Unay, S. Sayin, H. B. Yildiz, A. Cirpan and L. Toppare, *RSC Adv.*, 2015, **5**, 35940–35947.

113 F. N. Comba, M. R. Romero, F. S. Garay and A. M. Baruzzi, *Anal. Biochem.*, 2018, **550**, 34–40.

114 A. K. M. Kafi, M. Naqshabandi, M. M. Yusoff and M. J. Crossley, *Enzyme Microb. Technol.*, 2018, **113**, 67–74.

115 R. Y. A. Hassan, A. M. Kamel, M. S. Hashem, H. N. A. Hassan and M. A. Abd El-Ghaffar, *J. Solid State Electrochem.*, 2018, **22**, 1–7.

116 C. Kaçar, P. E. Erden and E. Kılıç, *Appl. Surf. Sci.*, 2017, **419**, 916–923.

117 S. Baluta, A. Lesiak and J. Cabaj, *Electroanalysis*, 2018, **30**, 1773–1782.

118 Y. Wang, F. Zhai, Y. Hasebe, H. Jia and Z. Zhang, *Bioelectrochemistry*, 2018, **122**, 174–182.

119 C. H. Díaz Nieto, A. M. Granero, J. C. Lopez, G. D. Pierini, G. J. Levin, H. Fernández and M. A. Zon, *Sens. Actuators, B*, 2018, **263**, 377–386.

120 Y. Wang, X. Liu, X. Xu, Y. Yang, L. Huang, Z. He, Y. Xu, J. Chen and Z. Feng, *Mater. Res. Bull.*, 2018, **101**, 340–346.

121 K. Saeedfar, L. Heng, T. Ling and M. Rezayi, *Sensors*, 2013, **13**, 16851–16866.

122 O. A. Biloivan, N. S. Rogaleva and Y. I. Korpan, *Biopolym. Cell*, 2010, **26**, 56–61.

123 S. Cogal, G. Celik Cogal and A. U. Oksuz, *Int. J. Polym. Mater. Polym. Biomater.*, 2018, **67**, 454–461.

124 V. A. Arlyapov, S. S. Kamanin, O. A. Kamanina and A. N. Reshetilov, *Nanotechnol. Russ.*, 2017, **12**, 658–666.

125 M. Romero-Arcos, M. G. Garnica-Romo and H. E. Martínez-Flores, *Procedia Technology*, 2017, **27**, 279–281.

126 S. R. Benjamin, R. S. Vilela, H. S. de Camargo, M. I. Guedes, F. Fernandes and F. Colmati, *Int. J. Electrochem. Sci.*, 2018, 563–586.

127 Z. L. Wu, Z. X. Liu and Y. H. Yuan, *J. Mater. Chem. B*, 2017, **5**, 3794–3809.

128 X. Sun and Y. Lei, *TrAC, Trends Anal. Chem.*, 2017, **89**, 163–180.

129 Y. Choi, Y. Choi, O.-H. Kwon and B.-S. Kim, *Chem.-Asian J.*, 2018, **13**, 586–598.

130 H. Shi, J. Wei, L. Qiang, X. Chen and X. Meng, *J. Biomed. Nanotechnol.*, 2014, **10**, 2677–2699.

131 Y. Su, X. Zhou, Y. Long and W. Li, *Microchim. Acta*, 2018, **185**, 114.

132 T. C. Canevari, F. H. Cincotto, D. Gomes, R. Landers and H. E. Toma, *Electroanalysis*, 2017, **29**, 1968–1975.

133 I. Vasilescu, S. A. V. Eremia, M. Kusko, A. Radoi, E. Vasile and G.-L. Radu, *Biosens. Bioelectron.*, 2016, **75**, 232–237.

134 S. Gupta, T. Smith, A. Banaszak and J. Boeckl, *Nanomaterials*, 2017, **7**, 301.

135 H. Razmi and R. Mohammad-Rezaei, *Biosens. Bioelectron.*, 2013, **41**, 498–504.

136 L. Tang, Y. Wang, Y. Li, H. Feng, J. Lu and J. Li, *Adv. Funct. Mater.*, 2009, **19**, 2782–2789.

137 S. Kumar, W. Ahlawat, R. Kumar and N. Dilbaghi, *Biosens. Bioelectron.*, 2015, **70**, 498–503.

138 S. Palanisamy, S. K. Ramaraj, S.-M. Chen, T. C. K. Yang, P. Yi-Fan, T.-W. Chen, V. Velusamy and S. Selvam, *Sci. Rep.*, 2017, **7**, 41214.

139 V. V. Neklyudov, N. R. Khafizov, I. A. Sedov and A. M. Dimiev, *Phys. Chem. Chem. Phys.*, 2017, **19**, 17000–17008.

140 J. A. Hondred, L. R. Stromberg, C. L. Mosher and J. C. Claussen, *ACS Nano*, 2017, **11**, 9836–9845.

141 A. Moya, G. Gabriel, R. Villa and F. Javier del Campo, *Curr. Opin. Electrochem.*, 2017, **3**, 29–39.

142 R. Ye, D. K. James and J. M. Tour, *Acc. Chem. Res.*, 2018, **51**, 1609–1620.

143 D. Vanegas, L. Patiño, C. Mendez, D. Oliveira, A. Torres, C. Gomes and E. McLamore, *Biosensors*, 2018, **8**, 42.

144 Z. Zhang, M. Song, J. Hao, K. Wu, C. Li and C. Hu, *Carbon*, 2018, **127**, 287–296.



145 M. Wang, X. Duan, Y. Xu and X. Duan, *ACS Nano*, 2016, **10**, 7231–7247.

146 M.-S. Chae, Y. K. Yoo, J. Kim, T. G. Kim and K. S. Hwang, *Sens. Actuators, B*, 2018, **272**, 448–458.

147 S. K. Bhardwaj, R. Chauhan, P. Yadav, S. Ghosh, A. K. Mahapatro, J. Singh and T. Basu, *Biomater. Sci.*, 2019, **7**, 1598–1606.

148 V. Perumal and U. Hashim, *J. Appl. Biomed.*, 2014, **12**, 1–15.

149 C. Lanzelotto, G. Favero, M. L. Antonelli, C. Tortolini, S. Cannistraro, E. Coppari and F. Mazzei, *Biosens. Bioelectron.*, 2014, **55**, 430–437.

150 A. Barberis, Y. Spissu, A. Fadda, E. Azara, G. Bazzu, S. Marceddu, A. Angioni, D. Sanna, M. Schirra and P. A. Serra, *Biosens. Bioelectron.*, 2015, **67**, 214–223.

151 M. Carano, S. Cosnier, K. Kordatos, M. Marcaccio, M. Margotti, F. Paolucci, M. Prato and S. Roffia, *J. Mater. Chem.*, 2002, **12**, 1996–2000.

152 L.-H. Lin and J.-S. Shih, *J. Chin. Chem. Soc.*, 2011, **58**, 228–235.

153 W. Zhilei, L. Zaijun, S. Xiulan, F. Yinjun and L. Junkang, *Biosens. Bioelectron.*, 2010, **25**, 1434–1438.

154 P. Piotrowski, K. Jakubow, B. Kowalewska and A. Kaim, *RSC Adv.*, 2017, **7**, 45634–45640.

155 R. N. Goyal, V. K. Gupta and N. Bachheti, *Anal. Chim. Acta*, 2007, **597**, 82–89.

156 J. A. Rather and K. De Wael, *Sens. Actuators, B*, 2013, **176**, 110–117.

157 R. N. N. Goyal, V. K. K. Gupta, N. Bachheti and R. A. A. Sharma, *Electroanalysis*, 2008, **20**, 757–764.

158 A. Ikeda and S. Shinkai, *Chem. Rev.*, 1997, **97**, 1713–1734.

159 N. Morohashi, F. Narumi, N. Iki, T. Hattori and S. Miyano, *Chem. Rev.*, 2006, **106**, 5291–5316.

160 D. O. Demirkol, H. B. Yildiz, S. Sayin and M. Yilmaz, *RSC Adv.*, 2014, **4**, 19900–19907.

161 O. Y. Saiapina, S. G. Kharchenko, S. G. Vishnevskii, V. M. Pyeshkova, V. I. Kalchenko and S. V. Dzyadevych, *Nanoscale Res. Lett.*, 2016, **11**, 105.

162 M. R. Karim, M. M. Alam, M. O. Aijaz, A. M. Asiri, M. A. Dar and M. M. Rahman, *Talanta*, 2019, **193**, 64–69.

163 M. Gerard, *Biosens. Bioelectron.*, 2002, **17**, 345–359.

164 N. Aydemir, J. Malmström and J. Travas-Sejdic, *Phys. Chem. Chem. Phys.*, 2016, **18**, 8264–8277.

165 B. Weng, A. Morrin, R. Shepherd, K. Crowley, A. J. Killard, P. C. Innis and G. G. Wallace, *J. Mater. Chem. B*, 2014, **2**, 793–799.

166 J. G. Ayenimo and S. B. Adeloju, *Food Chem.*, 2017, **229**, 127–135.

167 P. Krzyczmonik, E. Socha and S. Skrzypek, *Bioelectrochemistry*, 2015, **101**, 8–13.

168 S. Ivanova, Y. Ivanov and T. Godjevargova, *Open J. Appl. Biosens.*, 2013, **02**, 12–19.

169 E. Cevik, A. Cerit, N. Gazel and H. B. Yildiz, *Electroanalysis*, 2018, **30**, 2445–2453.

170 J. Ahmed, M. M. Rahman, I. A. Siddiquey, A. M. Asiri and M. A. Hasnat, *Electrochim. Acta*, 2017, **246**, 597–605.

171 M. M. Rahman, N. A. Alenazi, M. A. Hussein, M. M. Alam, K. A. Alamry and A. M. Asiri, *Mater. Res. Express*, 2018, **5**, 065019.

172 M. M. Hussain, M. M. Rahman and A. M. Asiri, *J. Environ. Sci.*, 2017, **53**, 27–38.

173 M. M. Rahman, J. Ahmed and A. M. Asiri, *RSC Adv.*, 2017, **7**, 14649–14659.

174 M. K. Alam, M. M. Rahman, M. Abbas, S. R. Torati, A. M. Asiri, D. Kim and C. Kim, *J. Electroanal. Chem.*, 2017, **788**, 66–73.

175 M. A. Hussein, M. M. Alam, N. A. Alenazi, K. A. Alamry, A. M. Asiri and M. M. Rahman, *J. Polym. Res.*, 2018, **25**, 262.

176 M. A. Daniele, M. Pedrero, S. Burrs, P. Chaturvedi, W. W. A. Wan Salim, F. Kuralay, S. Campuzano, E. McLamore, A. A. Cargill, S. Ding and J. C. Claussen, in *Nanobiosensors and Nanobioanalyses*, Springer, Japan, Tokyo, 2015, pp. 137–166.

177 M. F. Hossain and J. Y. Park, *PLoS One*, 2017, **12**, e0173553.

178 S. Morteza Naghib, *Int. J. Electrochem. Sci.*, 2018, 1013–1026.

179 D. H. Shin, W. Kim, J. Jun, J. S. Lee, J. H. Kim and J. Jang, *Sens. Actuators, B*, 2018, **264**, 216–223.

180 S. Kurbanoglu and S. A. Ozkan, *Electrocatalysis*, 2018, **9**, 252–257.

181 K. Varmira, G. Mohammadi, M. Mahmoudi, R. Khodarahmi, K. Rashidi, M. Hedayati, H. C. Goicoechea and A. R. Jalalvand, *Talanta*, 2018, **183**, 1–10.

182 N. Gan, X. Yang, D. Xie, Y. Wu and W. Wen, *Sensors*, 2010, **10**, 625–638.

183 M. C. Makel and J. A. Plucker, *Educ. Res.*, 2014, **43**, 304–316.

184 M. R. Munafò and G. Davey Smith, *Nature*, 2018, **553**, 399–401.

